A dual inhibitory mechanism sufficient to maintain cell cycle restricted CENP-A assembly

Ana Stankovic[1], Lucie Y. Guo[2], João F. Mata[1], Dani L. Bodor[1,6], Xing-Jun Cao[3], Aaron O. Bailey[4,7], Jeffrey Shabanowitz[5], Donald F. Hunt[5], Benjamin A. Garcia[3], Ben E. Black[2,] and Lars E.T Jansen[1,*]*

[1]Instituto Gulbenkian de Ciência, 2780-156 Oeiras, Portugal

[2]Department of Biochemistry and Biophysics, Perelman School of Medicine, University of Pennsylvania, Philadelphia, PA 19104, USA

[3]Epigenetics Program, Department of Biochemistry and Biophysics, Perelman School of Medicine, University of Pennsylvania, Philadelphia, PA 19104, USA

[4]Department of Cell Biology, University of Virginia, Charlottesville, VA, 22908, USA

[5]Department of Chemistry, University of Virginia, Charlottesville, VA, 22901 USA

[6]Current address: MRC Laboratory for Molecular Cell Biology, UCL, London WC1E 6BT, UK.

[7]Current Address: Thermo Fisher Scientific, San Jose, CA

[*]Co-corresponding authors

email:

Lars E.T. Jansen (Lead Contact): ljansen@igc.gulbenkian.pt

Ben E. Black: blackbe@mail.med.upenn.edu

Summary

Chromatin featuring the H3 variant CENP-A at the centromere is critical for its mitotic function and epigenetic maintenance. Assembly of centromeric chromatin is restricted to G1 phase through inhibitory action of Cdk1/2 kinases in other phases of the cell cycle. Here, we identify the two key targets sufficient to maintain cell cycle control of CENP-A assembly. We uncovered a single phosphorylation site in the licensing factor M18BP1 and a cyclin A binding site in the CENP-A chaperone, HJURP, mediating specific inhibitory phosphorylation. Simultaneous expression of mutant proteins lacking these residues, results in complete uncoupling from the cell cycle. Consequently, CENP-A assembly is fully recapitulated under high Cdk activities, indistinguishable from G1 assembly. We find that Cdk-mediated inhibition is exerted by sequestering active factors away from the centromere. Finally, we show that displacement of M18BP1 from the centromere is critical for the assembly mechanism of CENP-A.

Introduction

Centromeres are chromosomal loci that drive faithful genome segregation during mitotic division (Allshire and Karpen, 2008). The functional foundation of the centromere is established by a specialized chromatin structure that features the histone H3 variant CENP-A (Black and Cleveland, 2011). This CENP-A-based chromatin domain provides a structural platform for formation of the kinetochore which links chromosomes to spindle microtubules during mitosis (Cheeseman and Desai, 2008; Foltz et al., 2006; Okada et al., 2006). In addition, CENP-A ensures stable maintenance of centromere position through an epigenetic, self-propagating feedback loop (Black and Cleveland, 2011; Gómez-Rodríguez and Jansen, 2013). Support for the epigenetic nature of the centromere comes from naturally occurring neocentromeres (Amor et al., 2004; Marshall et al., 2008), where centromere proteins vacate the original centromeric DNA sequence and assemble heritably on previously naïve chromatin. In addition, ectopic targeting of CENP-A or proteins of the centromere complex to a non-centromeric locus was shown to be sufficient to initiate a functional and heritable centromere (Barnhart et al., 2011; Hori et al., 2013; Mendiburo et al., 2011). Consistent with a key role at the core of a positive epigenetic feedback loop, CENP-A nucleosomes are long lived and are maintained through multiple cell divisions (Bodor et al., 2013; Jansen et al., 2007). The unusually slow turnover of CENP-A at each centromere (Falk et al., 2015) indicates that replenishment is either equally slow or is limited in time and tied to CENP-A redistribution following DNA replication. Indeed, in metazoans, assembly of newly synthesized CENP-A is directly linked to cell cycle progression and is initiated during mitotic exit and restricted to early G1 phase of the cell cycle (Jansen et al., 2007; Schuh et al., 2007).

Previously we showed that brief inhibition of cyclin dependent kinase 1 and 2 (Cdk1/2) activities is sufficient to drive CENP-A deposition prior to mitotic exit (Silva et al., 2012). This has led to a model where the CENP-A assembly machinery is present and poised for activity but is kept inactive throughout S, G2 and M phase, until mitotic exit when activities of Cdk1/2 drop, concomitant with the onset of CENP-A deposition. Key proteins necessary for the process of CENP-A deposition include the Mis18 complex and the CENP-A chaperone HJURP which bears CENP-A-specific nucleosome assembly activity (Dunleavy et al., 2009; Foltz et al., 2009; Fujita et al., 2007). HJURP and M18BP1 (also known as HsKNL2), a member of the Mis18 complex, are phosphoproteins (Bailey et al., 2016; Dephoure et al., 2008; Kato et al., 2007; McKinley and Cheeseman, 2014; Müller et al., 2014; Silva et al., 2012; Wang et al., 2014) and localize to centromeres in a cell cycle controlled manner, in early G1 phase (Dunleavy et al., 2009; Foltz et al., 2009; Fujita et al., 2007; Maddox et al., 2007), indicating they are putative targets for Cdk regulation. In addition, recent work has identified the mitotic kinase Plk1 as a critical component to drive CENP-A assembly (McKinley and Cheeseman, 2014). However, while Plk1 is itself a cell cycle controlled kinase, it does not restrict CENP-A assembly to G1 phase as it is required for both canonical assembly in G1 phase as well as for premature assembly upon Cdk inhibition. In addition, several residues on CENP-A itself are phosphorylated (Bailey et al., 2016; Yu et al., 2015; Zeitlin et al., 2001). One of these, serine 68, is proposed to phosphorylated by mitotic Cdk activity (Yu et al., 2015) but the relevance of this is being disputed (Fachinetti et al., 2017) and mutation of this residue does not lead to a change in the timing of CENP-A deposition. In contrast, mutations of phospho-residues in HJURP or artificial recruitment of M18α to centromeres has been reported to result in premature centromere recruitment of CENP-A (McKinley and Cheeseman, 2014; Müller et al., 2014). While these studies point to a contributing role for these factors, they leave open the critical question of which factors are necessary, which are sufficient, how Cdk-mediated control is exerted, and how key proteins are functionally inhibited.

To resolve the specific molecular steps that ensure cell cycle restricted CENP-A assembly, we report full uncoupling of CENP-A assembly from the cell cycle/Cdk regulation. To achieve this, we identified a functional cyclin-interacting domain in HJURP and a critical phospho-site in M18BP1. Simultaneous uncoupling of these factors from cell cycle progression results in a complete reconstitution of CENP-A assembly process prematurely in G2 phase, prior to mitotic exit. Our results identify a dual inhibitory mechanism that is sufficient to maintain cell cycle restricted centromere propagation and define the molecular underpinnings of how assembly is turned on and subsequently turned off.

Results

HJURP is phosphorylated in a cell cycle dependent manner

HJURP, the CENP-A specific chaperone, is a phospho-protein and features several putative Cdk sites (Figure 1A and (Bailey et al., 2016; Dephoure et al., 2008; Kato et al., 2007; Müller et al., 2014; Wang et al., 2014), making it a prime candidate for cell cycle control of CENP-A assembly. To quantitatively measure HJURP phosphorylation we used stable isotope labeling by amino acids in cell culture (SILAC) coupled to mass spectrometry. This allowed us, in an unbiased manner, to precisely determine which residues are phosphorylated under high Cdk conditions and how these respond to changes in Cdk activity. Cdk1 levels differ most dramatically between mitosis and G1 phase. We therefore compared levels of phospho-peptides on the prenucleosomal GFP-CENP-A/HJURP complex between populations of mitotically arrested cells and cells that are released from mitotic arrest by Roscovitine-mediated Cdk inhibition (Figure 1B). Normal timing and efficiency of CENP-A assembly is preserved under these conditions (Figure S1). We detected 6 phosphorylated residues corresponding to putative Cdk consensus sites within HJURP, all of which were dephosphorylated upon mitotic exit, ranging from 25-70% decrease relative to mitotic values (Figures 1C, S2). Although three of these sites (S412, S448, S473) correspond to reported phospho-sites (Müller et al., 2014; Wang et al., 2014), our analysis shows that these are neither the sole nor the most responsive sites to inactivation of Cdks, at least in mitosis. In contrast, no change is observed at unphosphorylated peptides of HJURP (Figure 1C) nor at Cdk-consensus phospho-sites on the CENP-A N-terminal tail (Bailey et al., 2013) after forced mitotic exit (Figure 1D), indicating that protein levels of CENP-A and HJURP remain unaffected (see also Figure S1F, G) and that HJURP is selectively dephosphorylated.

The HJURP conserved domain interacts with Cyclin A and controls timing of CENP-A assembly

Our findings from SILAC experiments led us to focus on HJURP in particular, and determine how its phospho-regulation is coupled to the control of cell cycle timing of CENP-A chromatin assembly. Although the canonical consensus site for Cdks is (S/T)PX(K/R)(Hagopian et al., 2001; Holmes and Solomon, 1996), 5 of the 6 phospho-sites in HJURP that are affected by Cdk inactivation display a shorter (S/T)P motif (Figure 1A) (Errico et al., 2009). Phosphorylation of such truncated motifs often requires additional cyclin binding sites for enhanced substrate recognition (Adams et al., 1996; Russo et al., 1996). Indeed, we found a typical cyclin A binding RxL motif (Brown et al., 2007) within a vertebrate conserved domain (CD) of HJURP, which has no previously described function (Sanchez-Pulido et al., 2009). We tested whether HJURP interacts with cyclin A and B, the major drivers of Cdk activity in S/G2 phase and mitosis, respectively, all stages at which CENP-A assembly is inhibited (Silva et al., 2012). We performed either Cyclin B or Cyclin A co-immunoprecipitation from HEK293T cells in which we ectopically expressed either GFP-tagged HJURP with a mutated RxL motif (RLL>ALA, henceforth referred to as $HJURP^{AxA}$), or with a wild type CD. HJURP forms a homodimer (Zasadzińska et al., 2013). To avoid cross-dimerization with endogenous HJURP, we replaced its C-

terminal domain with that of LacI, which does not interfere with the CENP-A chaperoning and assembly activity of HJURP, as described (Zasadzińska et al., 2013) (henceforth named HJURP-ΔCLacI). Cyclin A robustly co-immunoprecipitated GFP-tagged HJURP-ΔCLacI (Figure 1E and supplemental Figure S3A). In contrast, GFP-HJURP^{AxA}-ΔCLacI pulldown was reduced by 70% compared to HJURP-ΔCLacI, carrying a wild type CD (Figure 1F). Mitotically enriched cells (low cyclin A) were used as a control to demonstrate that HJURP pulldown is cyclin A dependent. Consistent with the fact that inhibition of CENP-A assembly is maintained in mitosis (Jansen et al., 2007), even though cyclin A is degraded in early mitosis (den Elzen and Pines, 2001; Geley et al., 2001), we find that like cyclin A, cyclin B can interact with HJURP (Figure S3B). However, this interaction is not dependent on an intact CD within HJURP, indicating inhibitory control in mitosis is exerted through a different mechanism.

Our mapping of the principal cyclin A interaction site on HJURP allowed us to determine the consequences of the loss of this interaction for the timing of its localization along the cell cycle. Upon removal of soluble HJURP by pre-extraction we revealed that the stably chromatin bound, pre-mitotic HJURP-ΔCLacI is enriched in nucleoli [as observed previously (Dunleavy et al., 2009)]. In contrast, HJURP^{AxA}-ΔCLacI targeted to centromeres prematurely in G2 phase, the time of the cell cycle in which cyclin A is the principal cyclin (Figure 2A). In addition, we analyzed CENP-A deposition using a SNAP tag-based, fluorescent quench-chase-pulse labeling protocol that we described previously (Figure 2B)(Bodor et al., 2012; Silva et al., 2012). Remarkably, expression of the cyclin A binding mutant of HJURP, but not its wild type counterpart resulted in a precocious deposition of nascent CENP-A in G2 phase. We performed these experiments using HJURP-ΔCLacI to force homodimerization of HJURP^{AxA}. In this way, we show that HJURP^{AxA} itself is a functional assembly factor, independent of wildtype HJURP copies. Consistent with this, downregulation of endogenous HJURP showed no effect on either efficiency or frequency of premature CENP-A loading following GFP-HJURP^{AxA}–ΔCLacI expression (Figure S4A, B). Either GFP-HJURP^{AxA}–ΔCLacI (Figure 2B) or GFP-HJURP^{AxA} (carrying the endogenous C-terminal HJURP dimerization domain) (Figure 2B´´, S4C) expression result in a similar level of precocious deposition of CENP-A demonstrating that uncoupling is not an artifact of LacI mediated dimerization. Quantitative analysis showed that precocious CENP-A assembly at the centromere reached ~40% of G1 levels (Figure 2B, see also S4D)[i.e. 20% assembly per centromere, considering the replicated state of sister centromeres in G2 phase, unresolvable by microscopy]. We conclude that the CD of HJURP is a cell cycle control element that interacts with cyclin A. Disruption of this site is sufficient to alleviate at least part of the Cdk-mediated inhibition of HJURP.

Cdk activity controls HJURP localization not its chaperoning activity

Phosphorylation of HJURP could directly interfere with its chaperoning activity, thereby inactivating the key function of the protein. Alternatively, it may sequester an otherwise active HJURP away from the centromere, preventing its untimely recruitment. To distinguish between these possibilities, we fused HJURP to the DNA binding domain of CENP-B (CBdbd)(Figure 2C). This domain binds specifically to centromeric α-satellite DNA and allows us to drive HJURP to centromeres in G2 synchronized cells, while likely bearing inhibitory phosphorylation due to high Cdk activity. We detected nascent CENP-A-SNAP at G2 centromeres after expression of HJURP-CBdbd-GFP (Figure 2C, D) but not CBdbd-GFP alone, indicating centromeric localization of HJURP is sufficient to enable unscheduled CENP-A loading. Although HJURP is removed from mitotic chromatin (a process that apparently overrides the DNA binding activity of the CENP-B DNA binding domain), newly loaded CENP-A-SNAP remained associated with centromeres upon entry into mitosis, suggesting it is assembled into centromeric nucleosomes rather than part of an HJURP-associated prenucleosomal complex (Figure 2C, right). Based on these results, we conclude that Cdk-driven phosphorylation does not interfere with HJURP chaperoning activity, rather it results in sequestering HJURP away from the centromere, preventing its untimely recruitment.

HJURP Serine 210/211 is functionally phosphorylated in G2 phase cells

Next, we determined whether the uncoupling of HJURP from its cell cycle control involves specific phosphorylation sites. Expression of HJURP in which the 6 identified putative mitotic Cdk phospho-residues (Figure 1C) were mutated to alanine (either all 6 or combinations thereof) did not result in changes in the timing of CENP-A assembly (Figure S5B), despite previous reports implicating three of these residues [S412, S448, and S472 (Müller et al., 2014)]. Because we observe pre-mature CENP-A assembly in G2 phase during which cyclin A is the major cyclin, we aimed to identify additional, potentially relevant, phospho-residues in this cell cycle window. We expressed Doxycycline (Dox) inducible 3xFlag-HJURP-ΔCLacI or 3xFlag-HJURP^{AxA}-ΔCLacI in G2 phase enriched HeLa HILO cells (Khandelia et al., 2011)[Figure 3A, B (see also section below)]. Following 3xFlag-HJURP-ΔCLacI immunoprecipitation, TiO2 phospho-enrichment and mass spectrometry (Figure 3C), we identified S210/S211 phosphopeptides (the proximity of these residues prevented us from differentiating S210 vs. S211 as the site of phosphorylation). These phosphopeptides were not detected in mitotically synchronized cells (Figure 1C), suggesting differential phosphorylation of HJURP, consistent with our finding that cyclin B also interacts with HJURP but in a CD-independent manner (Figure S3B). Further, we found S412 to be the only common phospho-residue between G2 and mitotically synchronized cells (Figure 3F). Importantly, the relative abundance of S210/S211 phospho-peptides was substantially reduced on the HJURP^{AxA} mutant in which cyclin A binding is reduced compared to wild type (Figure 3E). This suggests that the cyclin A/Cdk complex interaction with HJURP results in phosphorylation of this site.

To test the functional significance of these residues we mutated serines 210 and 211 in combination with serine 412 and expressed HJURP^{S210A,S211A,S412A}-ΔCLacI mutants in G2 phase cells. Quench-chase-pulse labeling of CENP-A-SNAP showed that mutation of these residues to alanine results in low, but detectable levels of nascent CENP-A at centromeres (Figure 3G, H). This indicates that cyclin A binding to HJURP in G2 phase results in phosphorylation, at least on serines S210/211 and S412 and that these modifications contribute to preventing premature CENP-A assembly.

HJURP^{AxA}-induced CENP-A assembly in G2 phase is Mis18-dependent

Although HJURP^{AXA} is capable of inducing unscheduled CENP-A assembly, it does so with a relatively low efficiency and centromere specificity as compared to canonical G1 loading (Figure 2B´, B´´). This indicates that an additional level of cell cycle control exists. A candidate for this is the Mis18 complex, which includes Mis18α, Mis18β and the associated protein M18BP1 (Fujita et al., 2007). All subunits share a common localization pattern, with highly enriched and centromere specific localization in anaphase, followed by disappearance in mid-G1 (Fujita et al., 2007; Silva and Jansen, 2009). Interestingly, we found that premature, HJURP^{AXA} driven CENP-A assembly in G2 phase correlates with low levels of stably expressed GFP-Mis18α at centromeres (Figure 4A-C). Moreover, siRNA-mediated depletion of Mis18α leads to a loss of both canonical assembly in G1 phase as well as premature assembly of CENP-A in G2 phase (Figure 4D). This demonstrates that HJURP^{AxA}-induced assembly occurs through the canonical assembly pathway and suggests that the partial nature of this assembly is possibly due to low levels of Mis18 complex members at G2 centromeres.

Recruitment of the Mis18 complex to the centromere is controlled by phosphorylation of M18BP1^{T653}

Previously, we reported that a phospho-dead M18BP1 mutant in which 24 known phospho-sites are mutated to alanine, resulted in its premature centromere targeting (Silva et al., 2012), suggesting that at least one of these sites is regulated by Cdks. We now identified four putative Cdk motifs that are highly conserved among vertebrates, three of which are clustered close to the N-terminus of M18BP1 (T4, T40 and S110), while a fourth (T653) is located between the highly conserved SANTA and SANT domains (Maddox et al., 2007) (Figure 5A). Mutation of all 4 sites to alanine leads to a loss of cell cycle controlled localization of M18BP1 (Figure S6A). Interestingly, mutation of T653 alone was sufficient to result in premature centromere targeting of M18BP1 with a ~3-fold increase in centromeric levels relative to wild type protein (Figure 5B). We generated a phospho- and site-specific antibody against the T653 site and show that pT653 levels rise as cells accumulate in S/G2 and mitosis, correlating with increasing levels of Cdk1 and 2 activities (Figure 5C). A brief treatment with Cdk1/2 inhibitor of cells expressing GFP-

M18BP1 caused a strong reduction in phosphorylation of T653, suggesting that M18BP1 is a direct target of these kinases (Figure 5D).

Further, the M18BP1^{T653A} mutant co-recruited Mis18α to G2 centromeres, indicative of ongoing Mis18 complex formation independent of T653 phosphorylation (Figure S6B). An N-terminal 490 amino acid fragment of M18BP1 was reported to be functional in supporting CENP-A assembly in G1 phase (McKinley and Cheeseman, 2014), consistent with our finding that mutation of the T653 residue does not abrogate M18BP1 localization, but we now add that this residue controls cell cycle dependent localization. To test whether M18BP1 phosphorylation of T653 results in disruption of the Mis18α interaction, we expressed a translational fusion of wild type or mutant M18BP1 to the CBdbd in cells synchronized in G2 phase (analogous to artificial HJURP tethering, Figure 2C). Forced recruitment of M18BP1 to centromeres leads to strong co-recruitment of Mis18α to G2 centromeres, suggesting that the Mis18 complex can form under inhibitory Cdk activity, at least at this stage in the cell cycle (Figure S6C), although not in mitosis as observed previously (McKinley and Cheeseman, 2014). Similarly, forced recruitment of a phosphomimetic M18BP1^{T653D} (Figure S6C) or M18BP1^{T653E} (not shown) mutant is capable of co-recruitment of Mis18α. Thus, we find that mutation of the T653 residue does not disrupt the M18BP1/Mis18α interaction. Rather, its phosphorylation prevents centromere targeting of the Mis18 complex in G2 phase until mitotic exit when Cdk1/2 activities are low.

Cdk-mediated control of M18BP1 and HJURP is sufficient to ensure tight cell cycle timing of centromere propagation

Our results indicate that centromere localization of both HJURP and M18BP1 is blocked by Cdk-mediated phosphorylation, suggesting that combined phospho-control of these protein complexes contributes to cell cycle specific loading of CENP-A. To directly test this, we constructed HeLa HILO cells expressing equal levels of either HJURP-ΔCLacI or HJURP^{AxA}-ΔCLacI (Figure S7A) under the control of a doxycycline-inducible promoter at a defined locus using recombination-mediated cassette exchange (RMCE)(Khandelia et al., 2011). HJURP induction was performed either in cells stably expressing GFP-tagged M18BP1^{T653A} or expressing endogenous M18BP1 along with CENP-A-SNAP to assay for CENP-A assembly (Figure 6A). We compared the efficiency of G2 phase loading to the normal level of assembly in G1 phase. CENP-A assembly in uninduced control G1 cells was equal across all cell lines and essentially completed at the time of fixation (Figure S7B, C, respectively). As observed after transient expression, induction of HJURP^{AxA} alone resulted in low levels (~20% of G1, when corrected for centromere replication in G2 phase) of CENP-A assembly (Figure 6B, C, S7D). Force expression of otherwise wild type but GFP-tagged M18BP1 does not enhance the degree of premature CENP-A assembly (Figure S7E, E´). Conversely, constitutive M18BP1^{T653A} expression led to infrequent and inefficient recruitment of nascent CENP-A to G2 centromeres (Figure 6C).

Remarkably, induction of HJURP^{AxA} combined with stably expressed M18BP1^{T653A} resulted in highly efficient and centromere restricted CENP-A assembly in G2 phase, reaching 93% of G1 control levels (Figure 6C). In sum, while disrupting the timing of centromere targeting of either HJURP or M18BP1 results in a limited deregulation of CENP-A assembly, as has been shown previously (McKinley and Cheeseman, 2014; Müller et al., 2014), we now show that simultaneous uncoupling of both of these proteins leads to full-fledged CENP-A assembly, indistinguishable from canonical G1 phase assembly. These findings strongly suggest that M18BP1 and HJURP are the two principal targets of Cdk-mediated inhibition.

Efficient CENP-A assembly requires displacement of M18BP1 from the centromere

During the course of these experiments, we observed that induction of CENP-A assembly in G2 phase resulted in concomitant loss of centromeric GFP-M18BP1^{T653A} levels to under 30%, on average, relative to the uninduced control (Figure 6C, D). Expression of HJURP^{AxA}-ΔCLacI, but not wild-type HJURP results in GFP-M18BP1^{T653A} loss, showing that displacement is directly dependent on CENP-A assembly. This suggests that M18BP1 removal is an active, CENP-A loading-dependent process and not a passive consequence of cell cycle progression. To test this directly in G1 cells, we either over-expressed wild type M18BP1 or artificially tethered it to G1 centromeres (using the CBdbd tether) while measuring nascent CENP-A chromatin assembly (Figure 7A, B). We observe a ~40% reduction in nascent CENP-A fluorescent intensities in either of these conditions (Figure 7C). We conclude that while M18BP1 is an essential positive regulator of CENP-A assembly, preventing its turnover by overexpression or by rendering it unable to be removed from G1 centromeres results in defects in CENP-A assembly.

Discussion

We have identified the licensing factor M18BP1 and the CENP-A chaperone HJURP as the two key targets of Cdk-based inhibition sufficient for maintenance of strict cell cycle control of CENP-A assembly (Figure 7D). However, we do not exclude that additional levels of regulation exists, e.g. in chromatin maturation steps or in mitotic inhibition (which we find to be controlled in a distinct manner from G2 phase).

Inhibition of CENP-A assembly prior to mitosis at the level of HJURP or M18BP1 alone is incomplete. This is in agreement with previous studies that showed that mutation of HJURP phospho-sites within the HJURP C-Terminal Domain 1 (HCTD1)(Müller et al., 2014) or forced recruitment of Mis18α resulted in precocious CENP-A assembly (McKinley and Cheeseman, 2014). We note that in our system, mutation of the HCTD1 phosphosites did not result in precocious CENP-A assembly (Figure S5B). This discrepancy is likely the result of expression level differences between the cell types used in each study [Figure S5C and (Bodor et al., 2014)].

We provide evidence that the primary mechanism of Cdk-mediated inhibition is to prevent, otherwise active, factors from reaching the centromere (Figures 2C, S6B, C and 7D). We propose that phosphorylation blocks the ability of M18BP1 and HJURP to bind to a partner(s) already docked at the centromere. M18BP1 interacts with CENP-C which is a constitutive core component of the centromere (Dambacher et al., 2012; Hori et al., 2013; Moree et al., 2011; Nardi et al., 2016; Stellfox et al., 2016). In turn, the prenucleosomal HJURP/CENP-A complex binds to the Mis18 complex (Nardi et al., 2016; Wang et al., 2014). Our proposal is consistent with a recent report describing an interaction between HJURP and the Mis18 complex subunit Mis18β, that is reduced upon Cdk phosphorylation, *in vitro* (Wang et al., 2014).

Recent studies have reported cell cycle regulated phosphorylation of CENP-A itself (Yu et al., 2015) or Plk1-mediated modification of M18BP1 (McKinley and Cheeseman, 2014). While, the latter is required for Mis18 complex localization upon mitotic exit, none of these modifications directly dictates the G1 restricted CENP-A assembly. Therefore, while key positive regulatory events also involve phospho-regulation (which may include some of the novel phosphorylation sites that we identified on HJURP), we defined the specific targets and mechanisms of the inhibitory control that is responsible for limiting CENP-A assembly to G1 phase. Rather than relying on a single tightly regulated factor, the combinatorial action of two layers of control synergizes to efficiently restrict CENP-A assembly to early G1 phase.

The designation of the Mis18 complex as a priming (licensing) factor was originally inspired by its temporal centromere localization that initiates in anaphase, before the onset of CENP-A assembly (Fujita et al., 2007). This is analogous to licensing of DNA replication by the assembly of the pre-replication complex (pre-RC) in early G1 phase (Nishitani and Lygerou, 2002), the S-phase removal of which ensures a single round of genome duplication per cell cycle (Blow and Dutta, 2005; Blow and Hodgson, 2002). Analogously, we find that removal of M18BP1 from the centromere is directly coupled to the onset of CENP-A deposition, at least under induced conditions in G2 phase, providing a causal link between efficient CENP-A assembly and M18BP1 displacement from the centromere.

These results reveal novel parallels between DNA replication and CENP-A-chromatin, manifested in consumption of the licensing factor which is directly instigated by the start of duplication of the heritable mark. These findings are consistent with a recent study showing that nascent CENP-A/HJURP binding to the Mis18 complex in vitro leads to the disassembly of this complex (Nardi et al., 2016), suggesting that Mis18 complex disassembly could be a mechanism to turn off CENP-A chromatin assembly. We show that not only does CENP-A assembly result in Mis18 complex removal (as shown by (Nardi et al., 2016)) but that this is a requirement for efficient loading of CENP-A. Two possible implications follow from these observations. First, while M18BP1 is required for recruitment of nascent CENP-A to

centromeres, its presence may physically block completion of the assembly process. By direct binding to CENP-C (Dambacher et al., 2012; Moree et al., 2011; Shono et al., 2015; Westhorpe et al., 2015) which in turn interacts with CENP-A (Falk et al., 2015; Guse et al., 2011; Kato et al., 2013; Logsdon et al., 2015), it is possibly that M18BP1 physically marks the site of incorporation for nascent CENP-A. Inability to remove M18BP1 would therefore provoke steric inhibition, resulting in low rates of CENP-A incorporation. Secondly, given the key role in initiation of CENP-A loading, removal of M18BP1 from centromeres provides an ´´OFF´´ switch for the process of assembly, thereby contributing to a tight cell cycle window ensuring a single round of CENP-A incorporation per cell cycle.

Experimental Procedures

Cell synchronization

Double Thymidine-based synchronization was performed as described (Bodor et al., 2012). For Mitotic synchronization, 2,4 μM of EG5 inhibitor III Dimethylenastron-DMEIII (Calbiochem) was used for 24h. For synchronous mitotic exit, following DMEIII washout, HeLa and Hek293T were released for 5h and 7h, respectively. For Figure 2C, Nocodazole was used at 100ng/ml.

Co-Immunoprecipitation

HEK293T cells were transiently transfected with GFP-tagged constructs. 24h post-transfection cells were either allowed to continue to cycle or were treated overnight in DME III to induce mitotic arrest. Cells were harvested 48h post-transfection and subjected to cyclin A or B immunoprecipitation (See also supplemental experimental procedures). Isolated complexes were separated by SDS-PAGE followed by immunoblotting with anti-Cyclin A, (Figure 1E) or anti-Cyclin B (both Santa Cruz) (Figure S3B) and anti-GFP (Chromotek) antibodies and detected on an Odyssey near-infrared scanner and quantified using the Odyssey software (see also (Bodor et al., 2014)).

SILAC and affinity purification of prenucleosomal HJURP/CENP-A/H4 complex

SILAC labeling medium was supplemented with normal lysine and arginine (Sigma-Aldrich) for “light” medium, and 50 mg/ L $^{13}C_6$,$^{15}N_2$-lysine and 50 mg/L $^{13}C_6$,$^{15}N_4$-arginine (Silantes) for “heavy” medium (See also supplemental experimental procedures). Two parallel cultures of previously characterized HeLaS3 cells stably expressing (LAP)-tagged CENP-A (Bailey et al., 2013) were grown in either heavy or light medium until reaching ~98% labeling efficiency. To enrich for mitotic cells, both cultures were treated with 50 μM S-trityl-L-cysteine for 17 h. Subsequently, the "light" cells were treated with 100 μM R-Roscovitine (AdipoGen) for 30 min while the "heavy" cells were mock-treated with DMSO. Affinity purification of the prenucleosomal HJURP/CENP-A/H4 complexes from 1:1 mixed “light" and "heavy"

cells was performed as previously described (Bailey et al., 2013) except that protein elution was performed with 2% SDS and heating at 95°C.

Mass spectrometry and data analysis

Purified CENP-A and associated proteins were precipitated, washed and dried. Following reconstitution, proteins we cleaved with trypsin and phosphopeptides were enriched by TiO2 prior to mass spec analysis (See supplemental experimental procedures for details). Extracted-ion chromatograms (XICs) of each light and heavy peptide pair were used for quantification. L/H ratio represents the ratio of total area under each elution peak.

Affinity purification of 3XFlag-HJURP$^{wt/AxA}$-ΔCLacI and Mass spectrometry

HeLa HILO RMCE cell lines carrying either 3XFlag-HJURP-ΔCLacI or 3xFlag-HJURP^{AxA}-ΔCLacI were enriched in G2 phase as described (see cell synchronization) and induced with 10μg/ml of Doxycycline (Sigma) for 24h. HJURP was affinity purified using anti-Flag M2 mouse agarose beads (Sigma-Aldrich) as described (see Co-Immunoprecitation), followed by SDS-PAGE separation of bound complexes, staining (by Instant Blue, Expedeon) and subsequent HJURP band excision, in-gel trypsin digestion and phosphopeptide enrichment by TiO_2. Samples were run on a Q Exactive mass spectrometer coupled with Easy nLC 1000 HPLC. MaxQuant was used to search the human protein database and identify peptide sequences and extract their ion chromatograms.

SNAP Quench-Chase-Pulse Labeling

Cell lines expressing CENP-A-SNAP were pulse labeled as previously described (Bodor et al., 2012), with exception of HeLa HILO derived cell lines where BTP (New England Biolabs) concentration was adjusted to 0,5 μM.

Immunofluorescence and pre-extraction procedure

Procedures are essentially as described (Bodor et al., 2012) (See also supplemental experimental procedures). To detect GFP-HJURP^{AxA}-ΔCLacI on G2 centromeres, HeLa CENP-A-SNAP cells transiently expressing the construct were pre-extracted for 5min prior to fixation. Cells were counterstained using anti-CENP-T (Barnhart et al., 2011) and anti-Aurora B (1:100; BD transduction laboratories). GFP-HJURP^{AxA}-ΔCLacI signal was amplified using GFP-Booster Atto488 (Chromotek).

Microscopy

Imaging was performed using a DeltaVision Core system (Applied Precision) inverted microscope (Olympus, IX-71), coupled to a Cascade2 EMCCD camera (Photometrics). Images (1024x1024) were acquired at 1 x binning using a 100x oil objective (NA 1.40, UPlanSApo) with 0, 2 μm z sections.

Supplemental information

Supplemental Information includes Supplemental Experimental Procedures and 8 figures that can be found with this article online at XX.

Author contributions

AS performed the experiments. LYG performed CENP-A/HJURP co-purifications for SILAC experiments and helped write the manuscript. JFM generated constructs and performed experiments in Figure 4. DLB generated constructs for experiments in Figure 6 and S7. AOB, JS and DFH performed initial mass spec analysis of HJURP phosphorylation sites. LYG, XC, BEB and BAG performed mass-spec experiments and analysis. BEB helped write the manuscript. AS and LETJ conceived of the study and wrote the manuscript.

Acknowledgments

We thank N. Martins (IGC) for preliminary work on HJURP mutants, E.V. Makeyev NTU, Singapore and Dan Foltz (Northwestern University) for reagents, W. Siwek (IGC) for help with large scale cell culture, S. Muller and G. Almouzni (Curie) for reagents and help with pre-extraction procedure and T. Panchenko (UPenn) for guidance with culturing LAP-tagged CENP-A cells and helpful discussions. We thank Monica Bettencourt Dias, Alekos Athanasiadis, Raquel Oliveira and Jörg Becker (IGC) for critically reading the manuscript. Salary support to AS and DLB is provided by Fundação para a Ciência e a Tecnologia (FCT) fellowships SFRH/BD/51878/2012 and SFRH/BD/74284/2010, respectively and an "Investigador FCT" position to LETJ. This work is supported by NIH/NIGMS R01-GM082989 (BEB), NIH/NIGMS T32-GM008275 (UPenn Structural Biology and Molecular Biophysics Training Grant; supported LYG), NIH/NCI F30-CA186430 (LYG), NIH Grant GM 037537 (DFH) and GM 110174 (BAG). Work is further supported by the Fundação para a Ciência e a Tecnologia (FCT) grant BIA-BCM/100557/2008 (LETJ), an EMBO installation grant 1818 (LETJ) and an ERC-consolidator grant ERC-2013-CoG-615638 awarded to LETJ.

References

Adams, P.D., Sellers, W.R., Sharma, S.K., Wu, A.D., Nalin, C.M., and Kaelin, W.G. (1996). Identification of a cyclin-cdk2 recognition motif present in substrates and p21-like cyclin-dependent kinase inhibitors. Mol. Cell. Biol. *16*, 6623–6633.

Allshire, R.C., and Karpen, G.H. (2008). Epigenetic regulation of centromeric chromatin: old dogs, new tricks? Nat. Rev. Genet. *9*, 923–937.

Amor, D.J., Bentley, K., Ryan, J., Perry, J., Wong, L., Slater, H., and Choo, K.H.A. (2004). Human centromere repositioning "in progress." Proc. Natl. Acad. Sci. U. S. A. *101*, 6542–6547.

Bailey, A.O., Panchenko, T., Sathyan, K.M., Petkowski, J.J., Pai, P.-J., Bai, D.L., Russell,

D.H., Macara, I.G., Shabanowitz, J., Hunt, D.F., et al. (2013). Posttranslational modification of CENP-A influences the conformation of centromeric chromatin. Proc. Natl. Acad. Sci. *110*, 11827–11832.

Bailey, A.O., Panchenko, T., Shabanowitz, J., Lehman, S.M., Bai, D.L., Hunt, D.F., Black, B.E., and Foltz, D.R. (2016). Identification of the Post-translational Modifications Present in Centromeric Chromatin. Mol. Cell. Proteomics *15*, 918–931.

Barnhart, M.C., Kuich, P.H.J.L., Stellfox, M.E., Ward, J.A., Bassett, E.A., Black, B.E., and Foltz, D.R. (2011). HJURP is a CENP-A chromatin assembly factor sufficient to form a functional de novo kinetochore. J. Cell Biol. *194*, 229–243.

Black, B.E., and Cleveland, D.W. (2011). Epigenetic Centromere Propagation and the Nature of CENP-A Nucleosomes. Cell *144*, 471–479.

Blow, J.J., and Dutta, A. (2005). Preventing re-replication of chromosomal DNA. Nat. Rev. Mol. Cell Biol. *6*, 476–486.

Blow, J.J., and Hodgson, B. (2002). Replication licensing--defining the proliferative state? Trends Cell Biol. *12*, 72–78.

Bodor, D.L., Rodríguez, M.G., Moreno, N., and Jansen, L.E.T. (2012). Analysis of Protein Turnover by Quantitative SNAP-Based Pulse-Chase Imaging. Curr. Protoc. Cell Biol. *Chapter 8*, Unit8.8.

Bodor, D.L., Valente, L.P., Mata, J.F., Black, B.E., and Jansen, L.E.T. (2013). Assembly in G1 phase and long-term stability are unique intrinsic features of CENP-A nucleosomes. Mol. Biol. Cell *24*, 923–932.

Bodor, D.L., Mata, J.F., Sergeev, M., David, A.F., Salimian, K.J., Panchenko, T., Cleveland, D.W., Black, B.E., Shah, J. V., and Jansen, L.E.T. (2014). The quantitative architecture of centromeric chromatin. Elife *3*, 1–26.

Brown, N.R., Lowe, E.D., Petri, E., Skamnaki, V., Antrobus, R., and Johnson, L. (2007). Cyclin B and Cyclin A Confer Different Substrate Recognition Properties on CDK2. Cell Cycle *6*, 1350–1359.

Cheeseman, I.M., and Desai, A. (2008). Molecular architecture of the kinetochore-microtubule interface. Nat. Rev. Mol. Cell Biol. *9*, 33–46.

Dambacher, S., Deng, W., Hahn, M., Sadic, D., Fröhlich, J., Nuber, A., Hoischen, C., Diekmann, S., Leonhardt, H., and Schotta, G. (2012). CENP-C facilitates the recruitment of M18BP1 to centromeric chromatin. Nucleus *3*, 101–110.

Dephoure, N., Zhou, C., Villén, J., Beausoleil, S. a, Bakalarski, C.E., Elledge, S.J., and Gygi, S.P. (2008). A quantitative atlas of mitotic phosphorylation. Proc. Natl. Acad. Sci. U. S. A. *105*, 10762–10767.

Dunleavy, E.M., Roche, D., Tagami, H., Lacoste, N., Ray-Gallet, D., Nakamura, Y., Daigo, Y., Nakatani, Y., and Almouzni-Pettinotti, G. (2009). HJURP is a cell-cycle-dependent maintenance and deposition factor of CENP-A at centromeres. Cell *137*, 485–497.

den Elzen, N., and Pines, J. (2001). Cyclin A is destroyed in prometaphase and can delay chromosome alignment and anaphase. J. Cell Biol. *153*, 121–136.

Errico, A., Deshmukh, K., Tanaka, Y., Pozniakovsky, A., and Hunt, T. (2009).

Identification of substrates for cyclin dependent kinases. Adv. Enzyme Regul. *50*, 375–399.

Fachinetti, D., Logsdon, G.A., Amira, A., Selzer, E.B., Cleveland, D.W., and Black, B.E. (2017). CENP-A modifications on Ser68 and Lys124 are dispensable for establishment, maintenance, and long-term function of human centromeres. Dev. Cell *in press*.

Falk, S.J., Guo, L.Y., Sekulic, N., Smoak, E.M., Mani, T., Logsdon, G.A., Gupta, K., Jansen, L.E.T., Van Duyne, G.D., Vinogradov, S.A., et al. (2015). CENP-C reshapes and stabilizes CENP-A nucleosomes at the centromere. Science. *348*, 699–703.

Foltz, D.R., Jansen, L.E.T., Black, B.E., Bailey, A.O., Yates, J.R., and Cleveland, D.W. (2006). The human CENP-A centromeric nucleosome-associated complex. Nat. Cell Biol. *8*, 458–469.

Foltz, D.R., Jansen, L.E.T., Bailey, A.O., Yates, J.R., Bassett, E. a., Wood, S., Black, B.E., and Cleveland, D.W. (2009). Centromere-specific assembly of CENP-a nucleosomes is mediated by HJURP. Cell *137*, 472–484.

Fujita, Y., Hayashi, T., Kiyomitsu, T., Toyoda, Y., Kokubu, A., Obuse, C., and Yanagida, M. (2007). Priming of Centromere for CENP-A Recruitment by Human hMis18α, hMis18β, and M18BP1. Dev. Cell *12*, 17–30.

Geley, S., Kramer, E., Gieffers, C., Gannon, J., Peters, J.M., and Hunt, T. (2001). Anaphase-promoting complex/cyclosome-dependent proteolysis of human cyclin A starts at the beginning of mitosis and is not subject to the spindle assembly checkpoint. J. Cell Biol. *153*, 137–148.

Gómez-Rodríguez, M., and Jansen, L.E.T. (2013). Basic properties of epigenetic systems: lessons from the centromere. Curr. Opin. Genet. Dev. *23*, 219–227.

Guse, A., Carroll, C.W., Moree, B., Fuller, C.J., and Straight, A.F. (2011). In vitro centromere and kinetochore assembly on defined chromatin templates. Nature *477*, 354–358.

Hagopian, J.C., Kirtley, M.P., Stevenson, L.M., Gergis, R.M., Russo, A.A., Pavletich, N.P., Parsons, S.M., and Lew, J. (2001). Kinetic basis for activation of CDK2/cyclin A by phosphorylation. J. Biol. Chem. *276*, 275–280.

Holmes, J.K., and Solomon, M.J. (1996). A Predictive Scale for Evaluating Cyclin-dependent Kinase Substrates: A COMPARISON OF p34cdc2 AND p33cdk2. J. Biol. Chem. *271*, 25240–25246.

Hori, T., Shang, W.-H.H., Takeuchi, K., and Fukagawa, T. (2013). The CCAN recruits CENP-A to the centromere and forms the structural core for kinetochore assembly. J. Cell Biol. *200*, 45–60.

Jansen, L.E.T., Black, B.E., Foltz, D.R., and Cleveland, D.W. (2007). Propagation of centromeric chromatin requires exit from mitosis. J. Cell Biol. *176*, 795–805.

Kato, H., Jiang, J., Zhou, B.-R., Rozendaal, M., Feng, H., Ghirlando, R., Xiao, T.S., Straight, A.F., and Bai, Y. (2013). A Conserved Mechanism for Centromeric Nucleosome Recognition by Centromere Protein CENP-C. Science. *340*, 1110–1113.

Kato, T., Sato, N., Hayama, S., Yamabuki, T., Ito, T., Miyamoto, M., Kondo, S.,

Nakamura, Y., and Daigo, Y. (2007). Activation of Holliday junction recognizing protein involved in the chromosomal stability and immortality of cancer cells. Cancer Res. *67*, 8544–8553.

Khandelia, P., Yap, K., and Makeyev, E. V (2011). Streamlined platform for short hairpin RNA interference and transgenesis in cultured mammalian cells. Proc. Natl. Acad. Sci. U. S. A. *108*, 12799–12804.

Logsdon, G. a., Barrey, E.J., Bassett, E. a., DeNizio, J.E., Guo, L.Y., Panchenko, T., Dawicki-McKenna, J.M., Heun, P., and Black, B.E. (2015). Both tails and the centromere targeting domain of CENP-A are required for centromere establishment. J. Cell Biol. *208*, 521–531.

Maddox, P.S., Hyndman, F., Monen, J., Oegema, K., and Desai, A.B. (2007). Functional Genomics Identifies a Myb Domain–Containing Protein Family Required for Assembly of CENP-A Chromatin. J. Cell Biol. *176*, 757–763.

Marshall, O.J., Chueh, A.C., Wong, L.H., and Choo, K.H.A. (2008). Neocentromeres: New Insights into Centromere Structure, Disease Development, and Karyotype Evolution. Am. J. Hum. Genet. *82*, 261–282.

McKinley, K.L.L.L., and Cheeseman, I.M.M.M. (2014). Polo-like Kinase 1 Licenses CENP-A Deposition at Centromeres. Cell *158*, 397–411.

Mendiburo, M.J., Padeken, J., Fülöp, S., Schepers, A., and Heun, P. (2011). Drosophila CENH3 Is Sufficient for Centromere Formation. Science. *334*, 686–690.

Moree, B., Meyer, C.B., Fuller, C.J., and Straight, A.F. (2011). CENP-C recruits M18BP1 to centromeres to promote CENP-A chromatin assembly. J. Cell Biol. *194*, 855–871.

Müller, S., Montes de Oca, R., Lacoste, N., Dingli, F., Loew, D., Almouzni, G., Montes de Oca, R., Lacoste, N., Dingli, F., Loew, D., et al. (2014). Phosphorylation and DNA Binding of HJURP Determine Its Centromeric Recruitment and Function in CenH3(CENP-A) Loading. Cell Rep. *8*, 190–203.

Nardi, I.K.K., Zasadzińska, E., Stellfox, M.E.E., Knippler, C.M.M., and Foltz, D.R.R. (2016). Licensing of Centromeric Chromatin Assembly through the Mis18α-Mis18β Heterotetramer. Mol. Cell *61*, 774–787.

Nishitani, H., and Lygerou, Z. (2002). Control of DNA replication licensing in a cell cycle. Genes Cells *7*, 523–534.

Okada, M., Cheeseman, I.M., Hori, T., Okawa, K., McLeod, I.X., Yates, J.R. 3rd, Desai, A., and Fukagawa, T. (2006). The CENP-H–I complex is required for the efficient incorporation of newly synthesized CENP-A into centromeres. Nat. Cell Biol. *8*, 446–457.

Russo, A.A., Jeffrey, P.D., Patten, A.K., Massagué, J., and Pavletich, N.P. (1996). Crystal structure of the p27Kip1 cyclin-dependent-kinase inhibitor bound to the cyclin A-Cdk2 complex. Nature *382*, 325–331.

Sanchez-Pulido, L., Pidoux, A.L., Ponting, C.P., and Allshire, R.C. (2009). Common Ancestry of the CENP-A Chaperones Scm3 and HJURP. Cell *137*, 1173–1174.

Schuh, M., Lehner, C.F., and Heidmann, S. (2007). Incorporation of Drosophila

CID/CENP-A and CENP-C into Centromeres during Early Embryonic Anaphase. Curr. Biol. *17*, 237–243.

Shono, N., Ohzeki, J.-I., Otake, K., Martins, N.M.C., Nagase, T., Kimura, H., Larionov, V., Earnshaw, W.C., and Masumoto, H. (2015). CENP-C and CENP-I are key connecting factors for kinetochore and CENP-A assembly. J. Cell Sci. jcs.180786-.

Silva, M.C.C., and Jansen, L.E.T. (2009). At the right place at the right time: novel CENP-A binding proteins shed light on centromere assembly. Chromosoma *118*, 567–574.

Silva, M.C.C., Bodor, D.L., Stellfox, M.E., Martins, N.M.C., Hochegger, H., Foltz, D.R., and Jansen, L.E.T. (2012). Cdk Activity Couples Epigenetic Centromere Inheritance to Cell Cycle Progression. Dev. Cell *22*, 52–63.

Stellfox, M.E., Nardi, I.K., Knippler, C.M., and Foltz, D.R. (2016). Differential Binding Partners of the Mis18α/β YIPPEE Domains Regulate Mis18 Complex Recruitment to Centromeres. Cell Rep. 1–9.

Wang, J., Liu, X., Dou, Z., Chen, L., Jiang, H., Fu, C., Fu, G., Liu, D., Zhang, J., Zhu, T., et al. (2014). Mitotic Regulator Mis18β Interacts with and Specifies the Centromeric Assembly of Molecular Chaperone Holliday Junction Recognition Protein (HJURP). J. Biol. Chem. *289*, 8326–8336.

Westhorpe, F.G., Fuller, C.J., and Straight, A.F. (2015). A cell-free CENP-A assembly system defines the chromatin requirements for centromere maintenance. J. Cell Biol. jcb.201503132-.

Yu, Z., Zhou, X., Wang, W., Deng, W., Fang, J., Hu, H., Wang, Z., Li, S., Cui, L., Shen, J., et al. (2015). Dynamic Phosphorylation of CENP-A at Ser68 Orchestrates Its Cell-Cycle-Dependent Deposition at Centromeres. Dev. Cell *32*, 68–81.

Zasadzińska, E., Barnhart-Dailey, M.E.C., Kuich, P.H.J.L., and Foltz, D.R. (2013). Dimerization of the CENP-A assembly factor HJURP is required for centromeric nucleosome deposition. EMBO J. *32*, 2113–2124.

Zeitlin, S.G., Barber, C.M., Allis, C.D., and Sullivan, K. (2001). Differential regulation of CENP-A and histone H3 phosphorylation in G2/M. J. Cell Sci. *114*, 653–661.

Figure 1. HJURP is phosphorylated in a Cdk-dependent manner and interacts with cyclin A (related to Figures S1 and S2)

(A) Schematic representation of HJURP protein (Scm3: CENP-A binding domain; CD: Conserved Domain (CD), HCTD: (HJURP C-Terminal Domain). Position of phospho-sites identified by SILAC in C are indicated. Amino acid sequences flanking phospho-sites are annotated in grey.
(B) Schematic of SILAC experiment (see supplemental experimental procedures for details). Light cells were released into G1 by Roscovitine treatment for 30 min. At this stage HJURP is partially dephosphorylated (See Figure S1F, G).

(C) The L/H ratios of phosphorylated Cdk sites detected on endogenous HJURP are listed. A representative non-phosphorylated peptide (Np) is shown as internal control. Note: pS595 was detected on two independent peptides.

(D) L/H ratios of Cdk consensus sites within the N-terminal tail of CENP-A (See Figure S2 for data from two additional replicate experiments).

(E) HJURP CD mediates interaction with Cyclin A. (Top) Schematic representation of HJURP protein. Mutation of conserved RxL motif to AxA is annotated with black arrow. Experiments are performed with an HJURP construct in which the C-terminal homodimerization domain is replaced with that of LacI to prevent dimerization with wild type HJURP. (Bottom) co-IP of extracts expressing indicated constructs, either from asynchronous or mitotically enriched cells. Bound complexes were separated using SDS-PAGE followed by immunoblotting with indicated antibodies.

(F) Quantification of IP experiments. GFP signal from each IP was normalized to corresponding cyclin A signal and input GFP signal in order to control for IP efficiency and GFP fusion protein expression level, respectively. GFP-HJURP signals were set to 1. Error bars indicate SEM (standard error of mean) from 3 independent experiments.

Figure 2. Timing of HJURP targeting and CENP-A deposition is controlled by HJURP CD. (related to Figure S3 and S4)

(A) HeLa CENP-A-SNAP cells were transiently transfected with indicated constructs and Thymidine synchronized to enrich cells in G2 phase. Cells were permeabilized prior to fixation and counterstained for Aurora B, CENP-T and DAPI to distinguish between G2 and early G1 cell cycle phases, centromere localization and DNA, respectively. GFP booster was used to amplify GFP-HJURP fluorescent signal.

(B) Experiments were performed as in Figure 2A except here CENP-A assembly was assayed using SNAP TMR-labeling of its S phase synthesized pool. Following fixation, cells were counterstained for cyclin B and DAPI to indicate G2 status and DNA, respectively. (See Figure S4C for extended analysis of GFP-HJURP and GFP-HJURP^{AxA} induced assembly).

(B´) Left: Quantification of frequency of premature CENP-A loading in Cyclin B positive cells expressing GFP-HJURP^{AxA}-ΔCLacI. Right: Quantification of CENP-A-SNAP (TMR) fluorescent signal intensities of cells from experiment on the left in G2 phase (Cyclin B positive) and G1 phase (Cyclin B negative), using CENP-T signal as a centromere reference (not depicted). Centromeric CENP-A-SNAP fluorescent signals were normalized to average of G1 cells signals in each experiment (not considering the difference in replicated sister G2 centromeres vs. segregated G1 centromeres). 3 replicates, error bars indicate SEM.

(B``) Left: Quantification of frequency of premature CENP-A loading in Cyclin B positive cells expressing GFP-HJURP^{AxA} from 3 replicate experiments (see Figure S4C for images). Right: Quantification of CENP-A-SNAP (TMR) fluorescent signal intensities from the same experiment.

(C) Top: Schematic of relevant domains in centromere targeted HJURP. Bottom: HeLa CENP-A-SNAP cells were transfected with indicated constructs. 7 hours post Thymidine release cells were either fixed in G2 phase or collected in Nocodazole to enrich for mitotic cells. Cells were counterstained for cyclin B and DAPI to indicate G2 status and DNA, respectively.

(D) Quantification of frequency of premature CENP-A-SNAP deposition in Cyclin B positive cells, driven by expression of Cbdb-HJURP-GFP. Error bars indicate SEM.

Figure 3. HJURP Serine 210/211 is functionally phosphorylated in G2 phase cells. (related to Figure S5)

(A) Schematic of cell lines used for a label free mass spec analysis.

(B) HeLa HILO cells carrying indicated Doxycycline-inducible HJURP constructs were enriched in G2 cells by Thymidine arrest and release during Dox induction.

(C) Cell pellets obtained from experiment in (B) were subjected to immunoprecipitation using Flag-coupled agarose beads to isolate 3xFlag-HJURP-ΔCLacI, separated on SDS-PAGE followed by Coomassie-based excision of HJURP proteins. Purified proteins were subjected to trypsin digestion, phosho-peptide enrichment, followed by LC-MS/MS analysis.

(D) Mass spectra of a representative non-phosphorylated HJURP peptide from the flow through of the phospho-enrichment, of samples from cells containing WT HJURP-ΔCLacI (top) and HJURP^{AxA} -ΔCLacI (bottom).

(E) Mass spectra of the phosphopeptide containing pS210/pS211, from the elution of the phospho-enrichment from cells expressing indicated constructs. Because the two serines are adjacent, it was not possible to differentiate between S210 and S211 as the site of phosphorylation.

(F) Schematic representation of Cdk-consensus phospho-sites detected on HJURP in G2 phase.

(G) Experiment analogous to Figure 2A assaying indicated HJURP constructs for localization and CENP-A assembly in G2 phase.

(H) Representative images of cells from experiment in (G). CENP-A assembly was assayed using SNAP TMR-labeling of its S phase synthesized pool. Following fixation, cells were counterstained for cyclin B and DAPI to indicate G2 status and DNA, respectively.

(H´) Left: Quantification of frequency of premature CENP-A loading in Cyclin B positive cells expressing indicated constructs from 3 replicate experiments. Right: Quantification of CENP-A-SNAP (TMR) fluorescent signal intensities.

Figure 4. HJURP^{AxA} induced CENP-A assembly is Mis18α dependent.

(A) Stable GFP-Mis18α, CENP-A-SNAP double transgenic HeLa cells were transfected with untagged HJURP^{AxA}, synchronized and assayed for nascent CENP-A assembly by SNAP quench-chase-pulse labeling, followed by immunostaining for cyclin B and DAPI to indicate G2 status and DNA, respectively.

(B) Representative images of experiment described in (A).

(C) Quantification of frequency of CENP-A (TMR) positive G2 centromeres of experiment described in (A). Cells were scored in relation to whether GFP-M18α (green) or CENP-T (red) signals are simultaneously detected together with CENP-A (TMR) or not.

(D) Top: Scheme outlining RNAi against Mis18α or GAPDH, synchronization and Quench-Chase-Pulse labeling of CENP-A-SNAP, GFP-Mis18α cells. (Bottom) Quantification of CENP-A-SNAP (TMR) positive cells from 3 independent experiments. Error bars indicate SEM.

Figure 5. Cdk-mediated T653 phosphorylation of M18BP1 controls its centromere recruitment (related to Figure S6).

(A) M18BP1 T653 is conserved amongst vertebrates. Left: Schematic of M18BP1 protein. Relevant domains and conserved Cdk sites are indicated. Right: Conservation of human T653 residue across species. Conserved Threonine or Serine is highlighted in grey.

(B) T653 residue controls cell cycle-dependent M18BP1 centromere recruitment. Indicated constructs were transfected into asynchronous HeLa cells 48hr prior to fixation, followed by counterstaining for cyclin B, CENP-T and DAPI to indicate G2 status, centromeres and DNA, respectively.

(B´) Average centromeric GFP fluorescent signals from Cyclin B positive cells were determined using the Centromere Recognition and Quantification (CRaQ) method (Bodor et al., 2012) and normalized to GFP-M18BP1. Error bars indicate standard error of the mean (SEM) from 3 replicates.

(C) T653 is phosphorylated in a cell cycle dependent manner. Hek293T cells were transiently transfected with GFP-Mis18BP1 (WT) or GFP-Mis18BP1^{T653A} as a non-phosphorylatable control. 24h later, cells were synchronized in indicated cell cycle stages and lysed. Extracts were either left untreated or treated with lambda phosphatase, separated by SDS-PAGE followed by immunoblotting with indicated antibodies (see also supplemental experimental procedures). Apparent molecular weight is indicated. Cells were assayed for cell cycle position by FACS using propidium iodide (PI) to indicated DNA content.

(D) T653 is phosphorylated by Cdk1/2. Hek293T cells were transiently transfected with GFP-Mis18BP1 and enriched in G2 phase by a single thymidine block followed by 7h of release. 30min before fixation, cell were treated with 100μM Roscovitine. Extracts were separated by SDS-PAGE followed by immunoblotting with anti-GFP and anti-pT653 antibodies.

Figure 6. A dual inhibitory mechanism restricts CENP-A deposition to G1 phase (related to Figure S7).

(A) Schematic representation of Hela HILO cells carrying low levels of constitutively expressed CENP-A-SNAP (red), with or without stable expression of GFP M18BP1^{T653A} (green) along with Doxycycline-inducible 3xFlag-HJURP-ΔCLacI (blue) or 3xFlag-HJURP^{AxA}-ΔCLacI (purple). Cells were processes as indicated in the scheme.

(B) Representative images of the experiment described above. Following fixation, cells were counterstained for CENP-T and DAPI to indicate centromeres and DNA, respectively. Cell cycle status was determined by measuring total DAPI area (see supplemental experimental procedures).

(C) Quantification of CENP-A-SNAP fluorescent signals from (B). Average CENP-A-SNAP signals from G2 centromeres were normalized to respective G1 centromeres and corrected for centromere number (assuming signal intensity per focus represents 1 and 2 centromeres in G1 and G2, respectively). Error bars indicate SEM of 4 independent experiments.

(D) CENP-A assembly drives M18BP1 displacement from centromeres. Quantification of centromeric GFP-M18BP1^{T653A} fluorescent signals from (B) using CRaQ method. Average GFP-M18BP1^{T653A} signals were normalized to uninduced 3xFlag-HJURP-ΔCLacI expressing cells. Error bars indicate SEM of 4 independent experiments.

Figure 7. M18BP1 removal from G1 centromeres is necessary for efficient canonical CENP-A assembly

(A) HeLa CENP-A-SNAP cells were transfected with indicated constructs, and synchronized in mitosis by an overnight treatment with Eg5 inhibitor (DMEIII). Newly synthesized CENP-A pool was quenched in mitosis, followed by 5h of release in early G1 when nascent CENP-A-SNAP was labeled with TMR (G1 specific pool).

(B) Schematic of relevant domains in centromere targeted M18BP1.

(C) GFP positive cells were selected and CENP-A TMR fluorescent intensities were determined using CRaQ, with the exception of the untransfected control where all cell were analyzed.

(D) Model summarizing the key molecular steps that are sufficient to restrict CENP-A assembly to G1 phase. CD: HJURP vertebrate conserved domain.

Figure 1

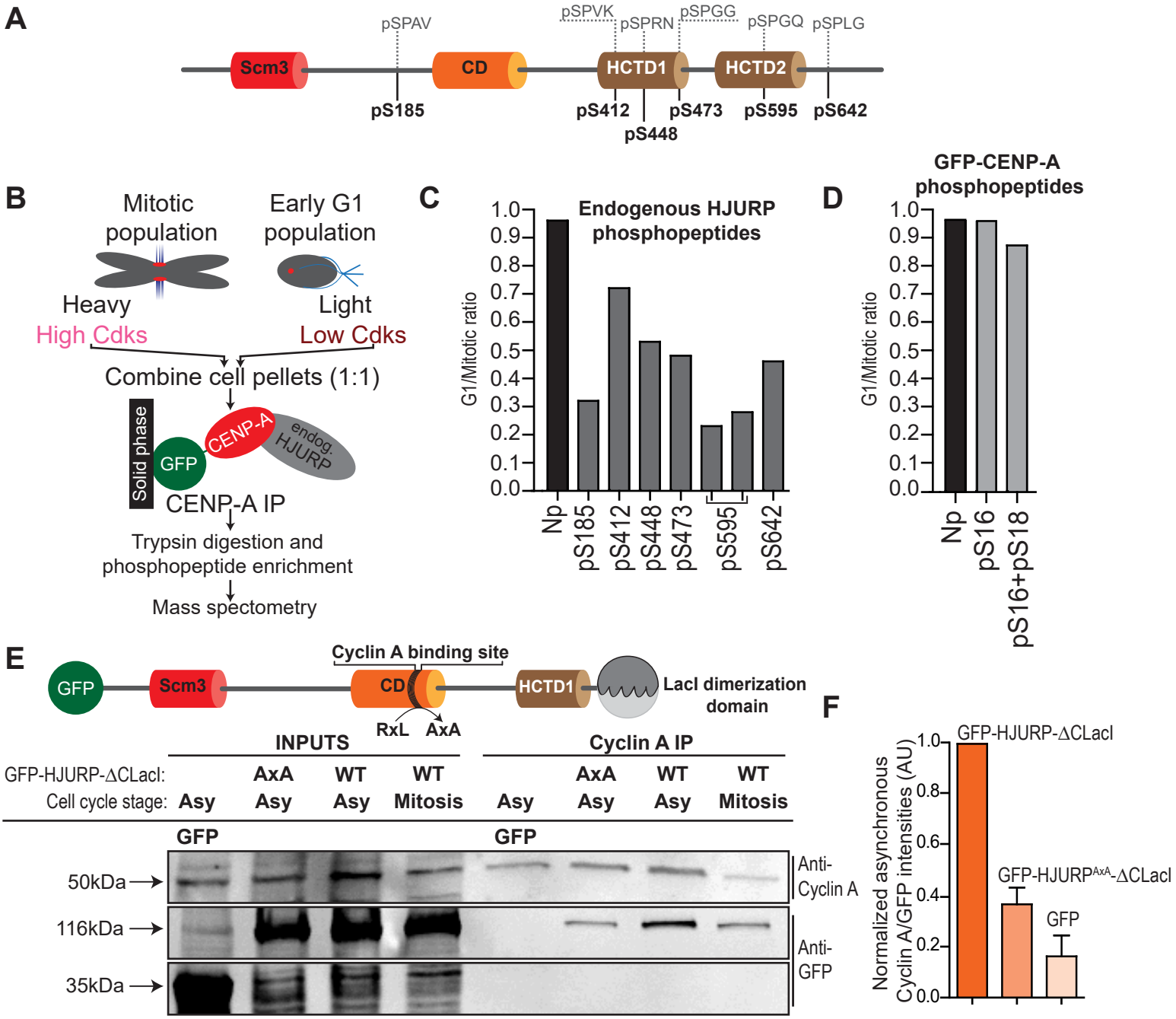
A
pSPAV
pSPVK
pSPRN
pSPGG
pSPGQ
pSPLG
Scm3
CD
HCTD1
HCTD2
pS185
pS412
pS448
pS473
pS595
pS642
B
Mitotic population
Early G1 population
Heavy
High Cdks
Light
Low Cdks
Combine cell pellets (1:1)
Solid phase
GFP
CENP-A
endog. HJURP
CENP-A IP
Trypsin digestion and phosphopeptide enrichment
Mass spectometry
C
Endogenous HJURP phosphopeptides
G1/Mitotic ratio
Np
pS185
pS412
pS448
pS473
pS595
pS642
D
GFP-CENP-A phosphopeptides
G1/Mitotic ratio
Np
pS16
pS16+pS18
E
GFP
Scm3
Cyclin A binding site
CD
RxL
AxA
HCTD1
LacI dimerization domain
INPUTS
Cyclin A IP
GFP-HJURP-ΔCLacI:
Cell cycle stage:
AxA
WT
WT
Asy
Asy
Asy
Mitosis
GFP
GFP
50kDa
116kDa
35kDa
Anti-Cyclin A
Anti-GFP
F
GFP-HJURP-ΔCLacI
GFP-HJURPAxA-ΔCLacI
GFP
Normalized asynchronous Cyclin A/GFP intensities (AU)

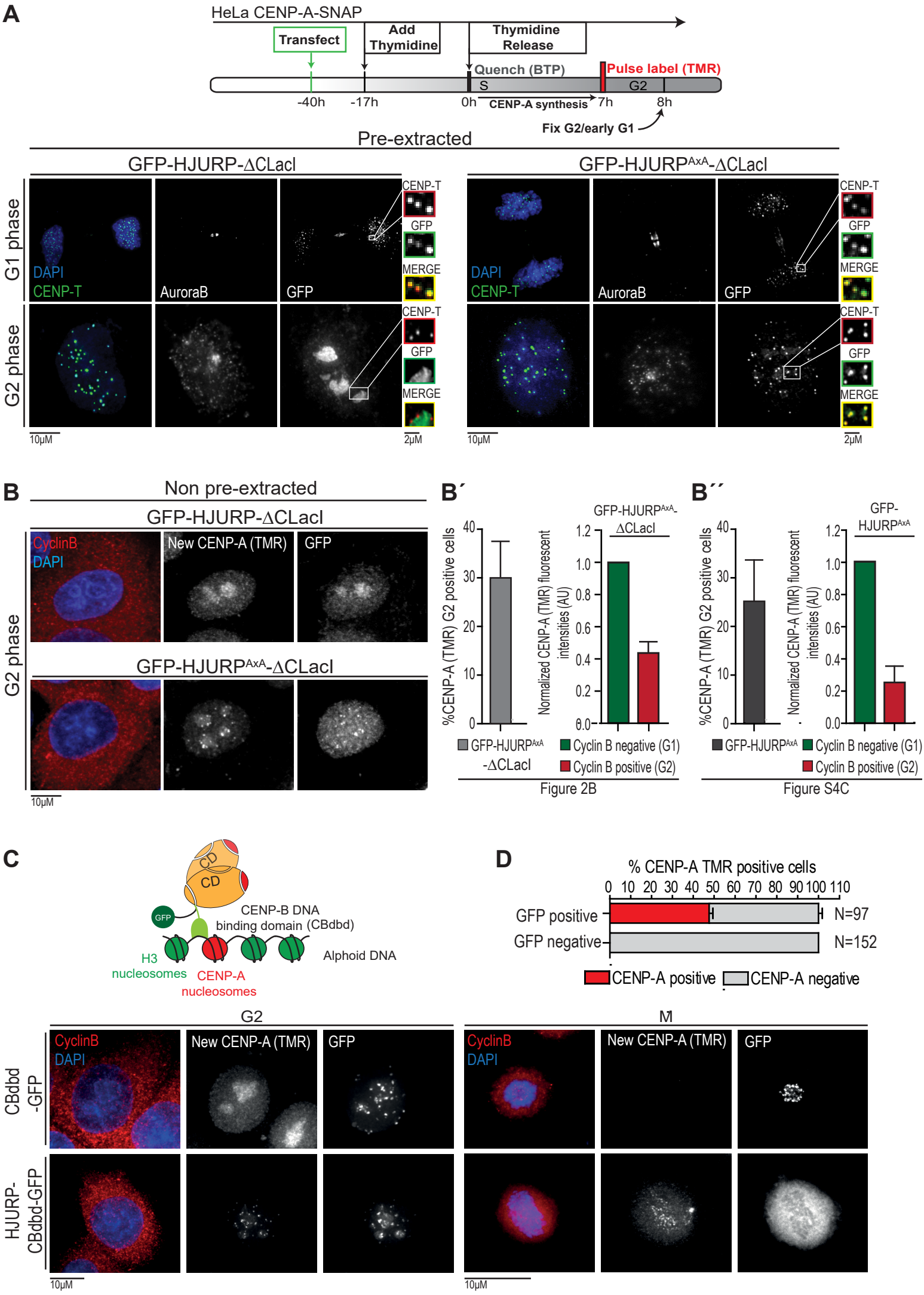
A
HeLa CENP-A-SNAP
Transfect
Add Thymidine
Thymidine Release
Quench (BTP)
Pulse label (TMR)
S
G2
-40h
-17h
0h
CENP-A synthesis
7h
8h
Fix G2/early G1
Pre-extracted
GFP-HJURP-ΔCLacI
GFP-HJURPAxA-ΔCLacI
G1 phase
G2 phase
DAPI
CENP-T
AuroraB
GFP
MERGE
10μM
2μM
B
Non pre-extracted
GFP-HJURP-ΔCLacI
GFP-HJURPAxA-ΔCLacI
CyclinB
DAPI
New CENP-A (TMR)
GFP
G2 phase
10μM
B´
%CENP-A (TMR) G2 positive cells
Normalized CENP-A (TMR) fluorescent intensities (AU)
GFP-HJURPAxA-ΔCLacI
Cyclin B negative (G1)
Cyclin B positive (G2)
Figure 2B
B´´
GFP-HJURPAxA
Figure S4C
C
CD
GFP
CENP-B DNA binding domain (CBdbd)
H3 nucleosomes
CENP-A nucleosomes
Alphoid DNA
D
% CENP-A TMR positive cells
GFP positive
GFP negative
N=97
N=152
CENP-A positive
CENP-A negative
G2
M
CBdbd-GFP
HJURP-CBdbd-GFP

Figure 3

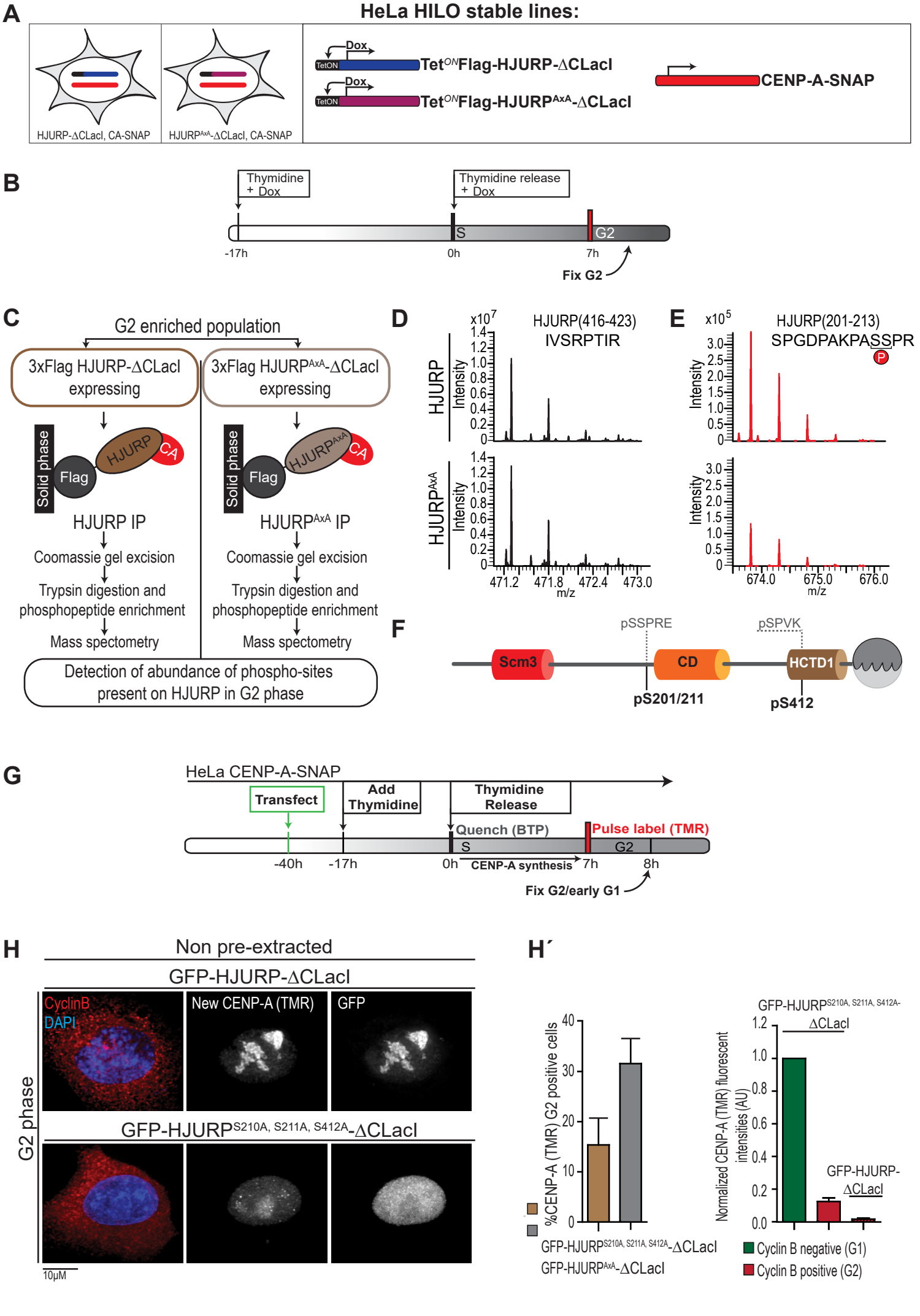
A
HeLa HILO stable lines:
HJURP-ΔCLaclI, CA-SNAP
HJURPAxA-ΔCLaclI, CA-SNAP
Dox
TetON
TetONFlag-HJURP-ΔCLaclI
Dox
TetON
TetONFlag-HJURPAxA-ΔCLaclI
CENP-A-SNAP
B
Thymidine + Dox
Thymidine release + Dox
S
G2
-17h
0h
7h
Fix G2
C
G2 enriched population
3xFlag HJURP-ΔCLaclI expressing
3xFlag HJURPAxA-ΔCLaclI expressing
Solid phase
Flag
HJURP
CA
HJURPAxA
HJURP IP
HJURPAxA IP
Coomassie gel excision
Trypsin digestion and phosphopeptide enrichment
Mass spectometry
Detection of abundance of phospho-sites present on HJURP in G2 phase
D
HJURP(416-423)
IVSRPTIR
HJURP
HJURPAxA
Intensity
x10^7
m/z
E
HJURP(201-213)
SPGDPAKPASSPR
P
x10^5
Intensity
m/z
F
pSSPRE
pSPVK
Scm3
CD
HCTD1
pS201/211
pS412
G
HeLa CENP-A-SNAP
Transfect
Add Thymidine
Thymidine Release
Quench (BTP)
Pulse label (TMR)
S
G2
-40h
-17h
0h
CENP-A synthesis
7h
8h
Fix G2/early G1
H
Non pre-extracted
GFP-HJURP-ΔCLaclI
CyclinB
DAPI
New CENP-A (TMR)
GFP
G2 phase
GFP-HJURPS210A, S211A, S412A-ΔCLaclI
10μM
H´
%CENP-A (TMR) G2 positive cells
GFP-HJURPS210A, S211A, S412A-ΔCLaclI
GFP-HJURPAxA-ΔCLaclI
GFP-HJURPS210A, S211A, S412A-ΔCLaclI
Normalized CENP-A (TMR) fluorescent intensities (AU)
GFP-HJURP-ΔCLaclI
Cyclin B negative (G1)
Cyclin B positive (G2)

Figure 4

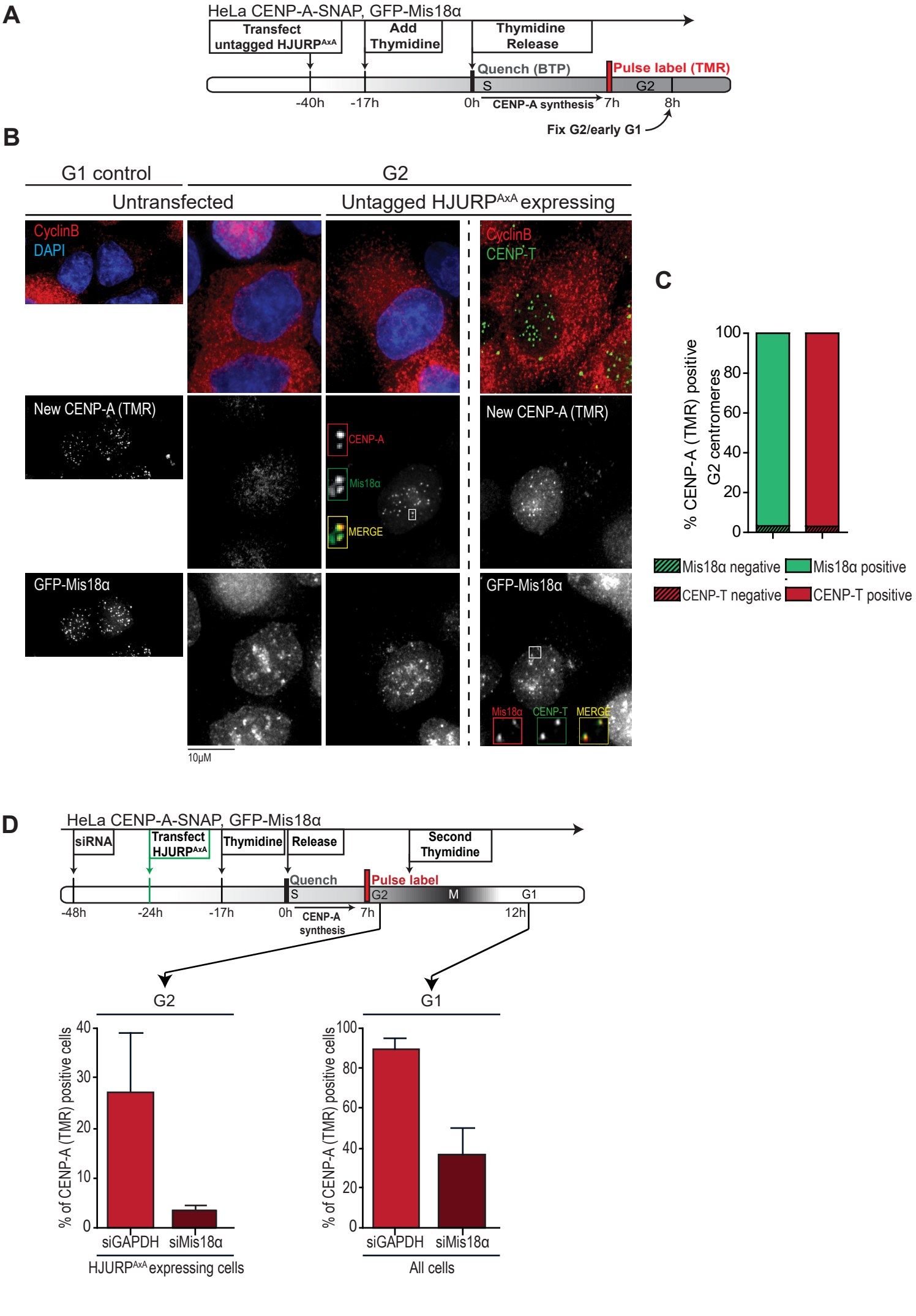
A
HeLa CENP-A-SNAP, GFP-Mis18α
Transfect untagged HJURP^AxA
Add Thymidine
Thymidine Release
Quench (BTP)
Pulse label (TMR)
S
G2
-40h
-17h
0h
CENP-A synthesis
7h
8h
Fix G2/early G1
B
G1 control
G2
Untransfected
Untagged HJURP^AxA expressing
CyclinB
DAPI
CyclinB
CENP-T
New CENP-A (TMR)
CENP-A
Mis18α
MERGE
New CENP-A (TMR)
GFP-Mis18α
GFP-Mis18α
Mis18α
CENP-T
MERGE
10μM
C
% CENP-A (TMR) positive G2 centromeres
100
80
60
40
20
0
Mis18α negative
Mis18α positive
CENP-T negative
CENP-T positive
D
HeLa CENP-A-SNAP, GFP-Mis18α
siRNA
Transfect HJURP^AxA
Thymidine
Release
Second Thymidine
Quench
Pulse label
S
G2
M
G1
-48h
-24h
-17h
0h
CENP-A synthesis
7h
12h
G2
G1
% of CENP-A (TMR) positive cells
40
30
20
10
0
siGAPDH
siMis18α
HJURP^AxA expressing cells
% of CENP-A (TMR) positive cells
100
80
60
40
20
0
siGAPDH
siMis18α
All cells

Figure 5

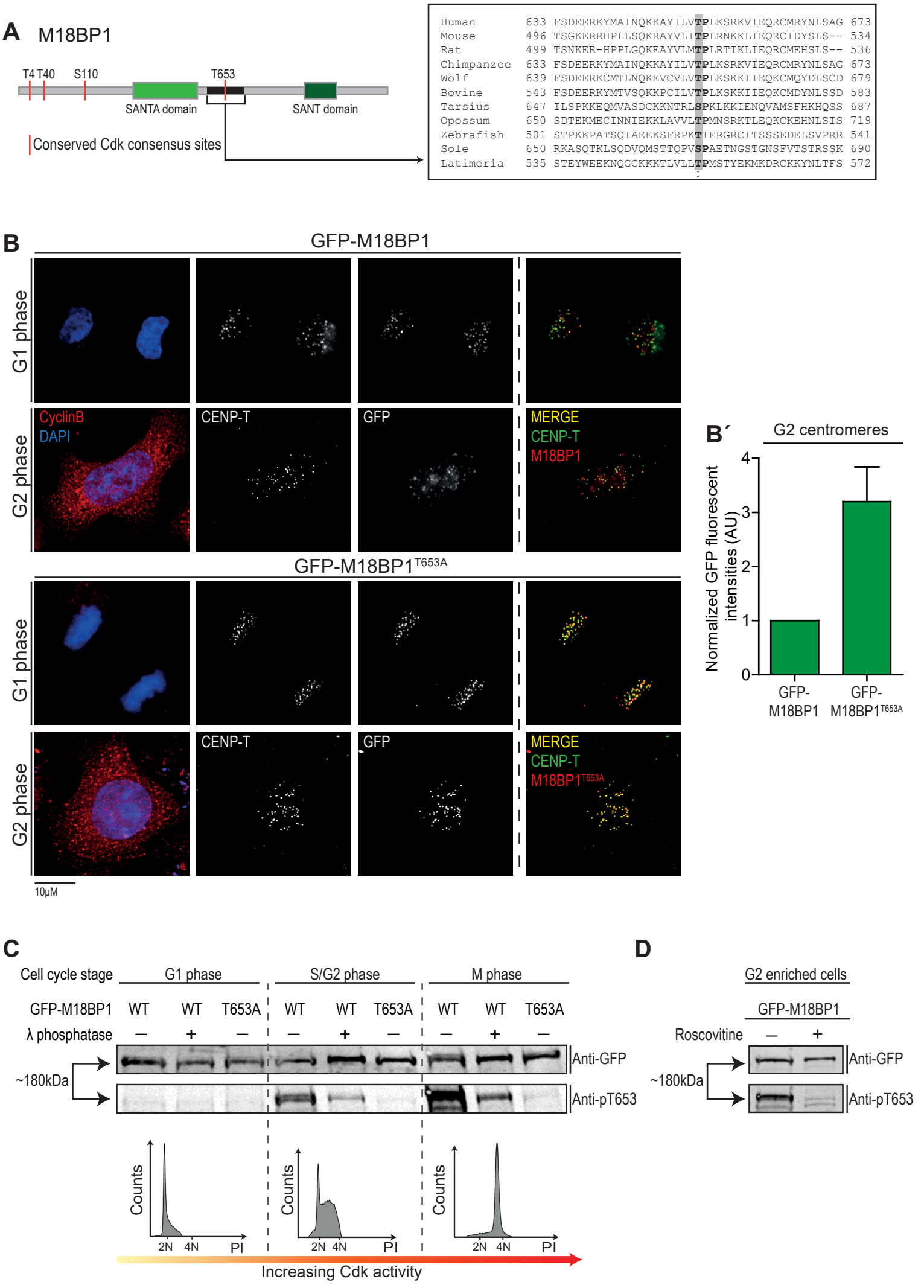
A
M18BP1
T4 T40
S110
T653
SANTA domain
SANT domain
Conserved Cdk consensus sites
Human 633 FSDEERKYMAINQKKAYILVTPLKSRKVIEQRCMRYNLSAG 673
Mouse 496 TSGKERRHPLLSQKRAYVLITPLRNKKLIEQRCIDYSLS-- 534
Rat 499 TSNKER-HPPLGQKEAYVLMTPLRTTKLIEQRCMEHSLS-- 536
Chimpanzee 633 FSDEERKYMAINQKKAYILVTPLKSRKVIEQRCMRYNLSAG 673
Wolf 639 FSDEERKCMTLNQKEVCVLVTPLKSKKIIEQKCMQYDLSCD 679
Bovine 543 FSDEERKYMTVSQKKPCILVTPLKSKKIIEQKCMDYNLSSD 583
Tarsius 647 ILSPKKEQMVASDCKKNTRLSPKLKKIENQVAMSFHKHQSS 687
Opossum 650 SDTEKMECINNIEKKLAVVLTPMNSRKTLEQKCKEHNLSIS 719
Zebrafish 501 STPKKPATSQIAEEKSFRPKTIERGRCITSSSEDELSVPRR 541
Sole 650 RKASQTKLSQDVQMSTTQPVSPAETNGSTGNSFVTSTRSSK 690
Latimeria 535 STEYWEEKNQGCKKKTLVLLTPMSTYEKMKDRCKKYNLTFS 572
B
GFP-M18BP1
G1 phase
G2 phase
CyclinB
DAPI
CENP-T
GFP
MERGE
CENP-T
M18BP1
GFP-M18BP1T653A
MERGE
CENP-T
M18BP1T653A
10µM
B´
G2 centromeres
Normalized GFP fluorescent intensities (AU)
0
1
2
3
4
GFP-M18BP1
GFP-M18BP1T653A
C
Cell cycle stage
G1 phase
S/G2 phase
M phase
GFP-M18BP1
WT
WT
T653A
λ phosphatase
~180kDa
Anti-GFP
Anti-pT653
Counts
2N 4N PI
Increasing Cdk activity
D
G2 enriched cells
GFP-M18BP1
Roscovitine
~180kDa
Anti-GFP
Anti-pT653

Figure 6

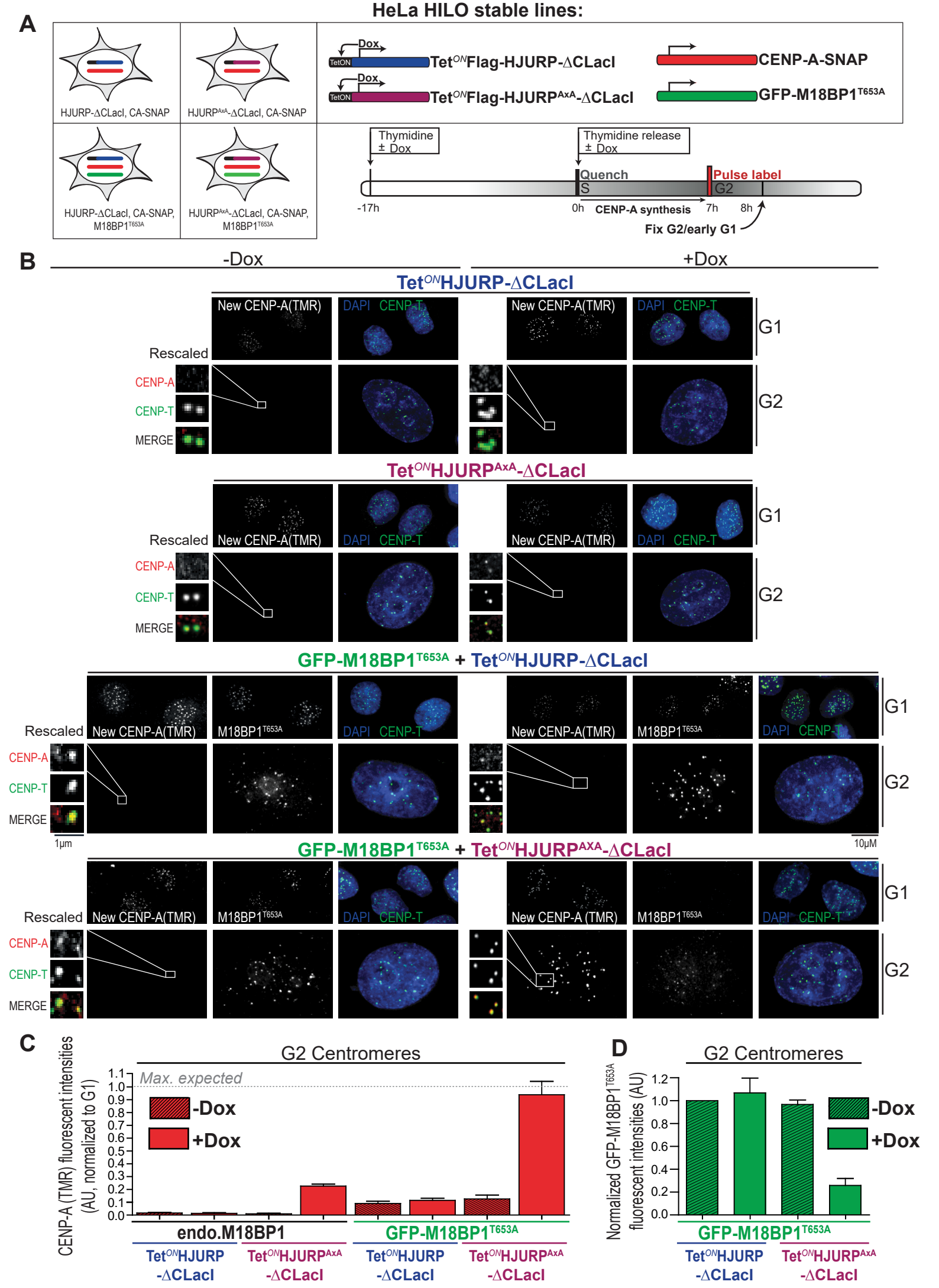
A
HeLa HILO stable lines:
HJURP-ΔCLacI, CA-SNAP
HJURPAxA-ΔCLacI, CA-SNAP
HJURP-ΔCLacI, CA-SNAP, M18BP1T653A
HJURPAxA-ΔCLacI, CA-SNAP, M18BP1T653A
Dox
TetON
TetONFlag-HJURP-ΔCLacI
TetONFlag-HJURPAxA-ΔCLacI
CENP-A-SNAP
GFP-M18BP1T653A
Thymidine ± Dox
Thymidine release ± Dox
Quench
Pulse label
S
G2
-17h
0h
CENP-A synthesis
7h
8h
Fix G2/early G1
B
-Dox
+Dox
TetONHJURP-ΔCLacI
TetONHJURPAxA-ΔCLacI
GFP-M18BP1T653A + TetONHJURP-ΔCLacI
GFP-M18BP1T653A + TetONHJURPAXA-ΔCLacI
Rescaled
New CENP-A(TMR)
M18BP1T653A
DAPI CENP-T
CENP-A
CENP-T
MERGE
G1
G2
1μm
10μM
C
G2 Centromeres
CENP-A (TMR) fluorescent intensities (AU, normalized to G1)
Max. expected
-Dox
+Dox
endo.M18BP1
GFP-M18BP1T653A
TetONHJURP -ΔCLacI
TetONHJURPAxA -ΔCLacI
D
G2 Centromeres
Normalized GFP-M18BP1T653A fluorescent intensities (AU)
-Dox
+Dox
GFP-M18BP1T653A
TetONHJURP -ΔCLacI
TetONHJURPAxA -ΔCLacI

Figure 7

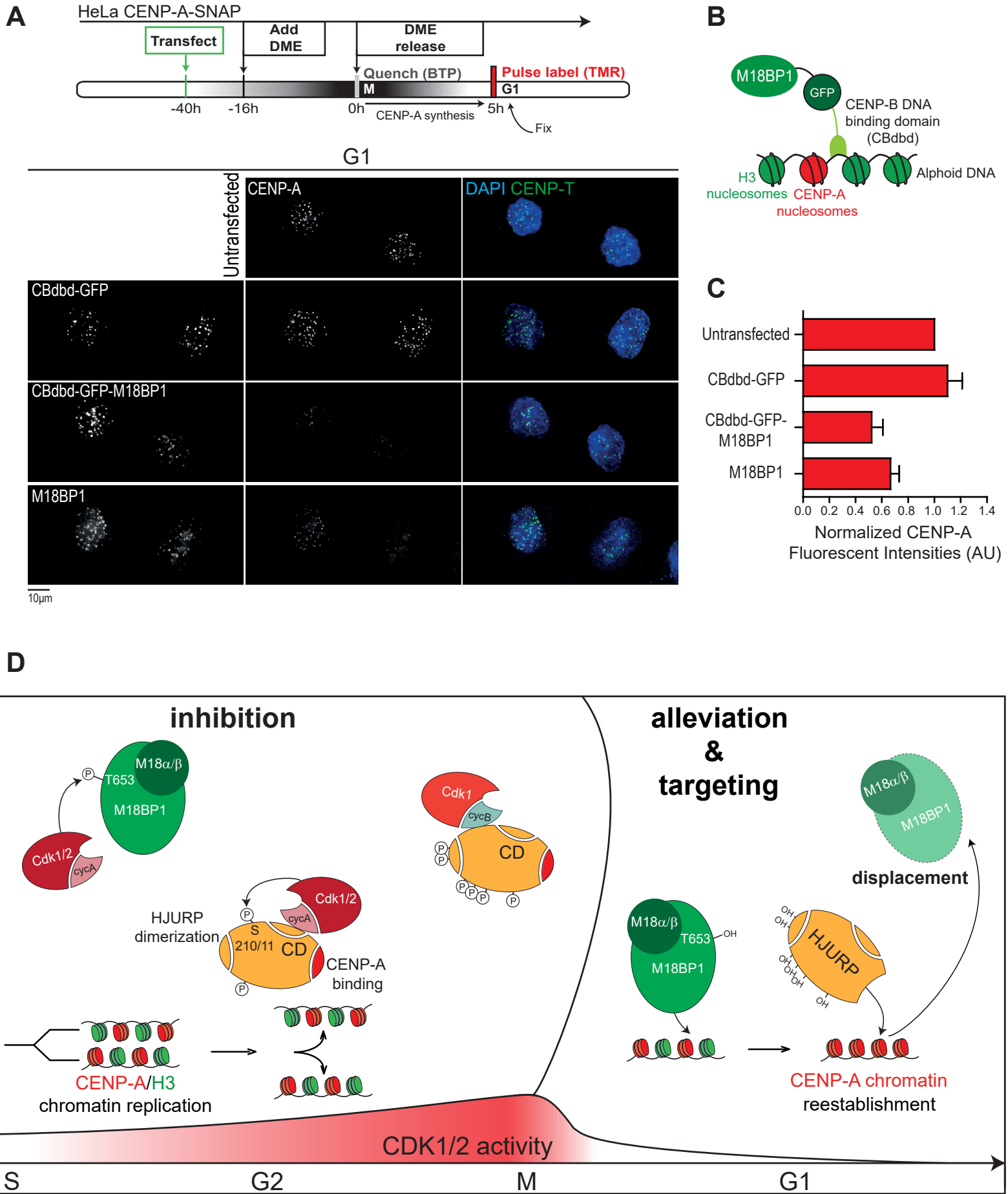
A
HeLa CENP-A-SNAP
Transfect
Add DME
DME release
Quench (BTP)
Pulse label (TMR)
M
G1
-40h
-16h
0h
CENP-A synthesis
5h
Fix
G1
Untransfected
CENP-A
DAPI CENP-T
CBdbd-GFP
CBdbd-GFP-M18BP1
M18BP1
10μm
B
M18BP1
GFP
CENP-B DNA binding domain (CBdbd)
H3 nucleosomes
CENP-A nucleosomes
Alphoid DNA
C
Untransfected
CBdbd-GFP
CBdbd-GFP-M18BP1
M18BP1
0.0 0.2 0.4 0.6 0.8 1.0 1.2 1.4
Normalized CENP-A Fluorescent Intensities (AU)
D
inhibition
M18α/β
T653
M18BP1
Cdk1/2
cycA
Cdk1
cycB
CD
HJURP dimerization
S 210/11
CENP-A binding
CENP-A/H3 chromatin replication
alleviation & targeting
displacement
HJURP
CENP-A chromatin reestablishment
CDK1/2 activity
S
G2
M
G1

Supplemental Information

Supplemental Figures

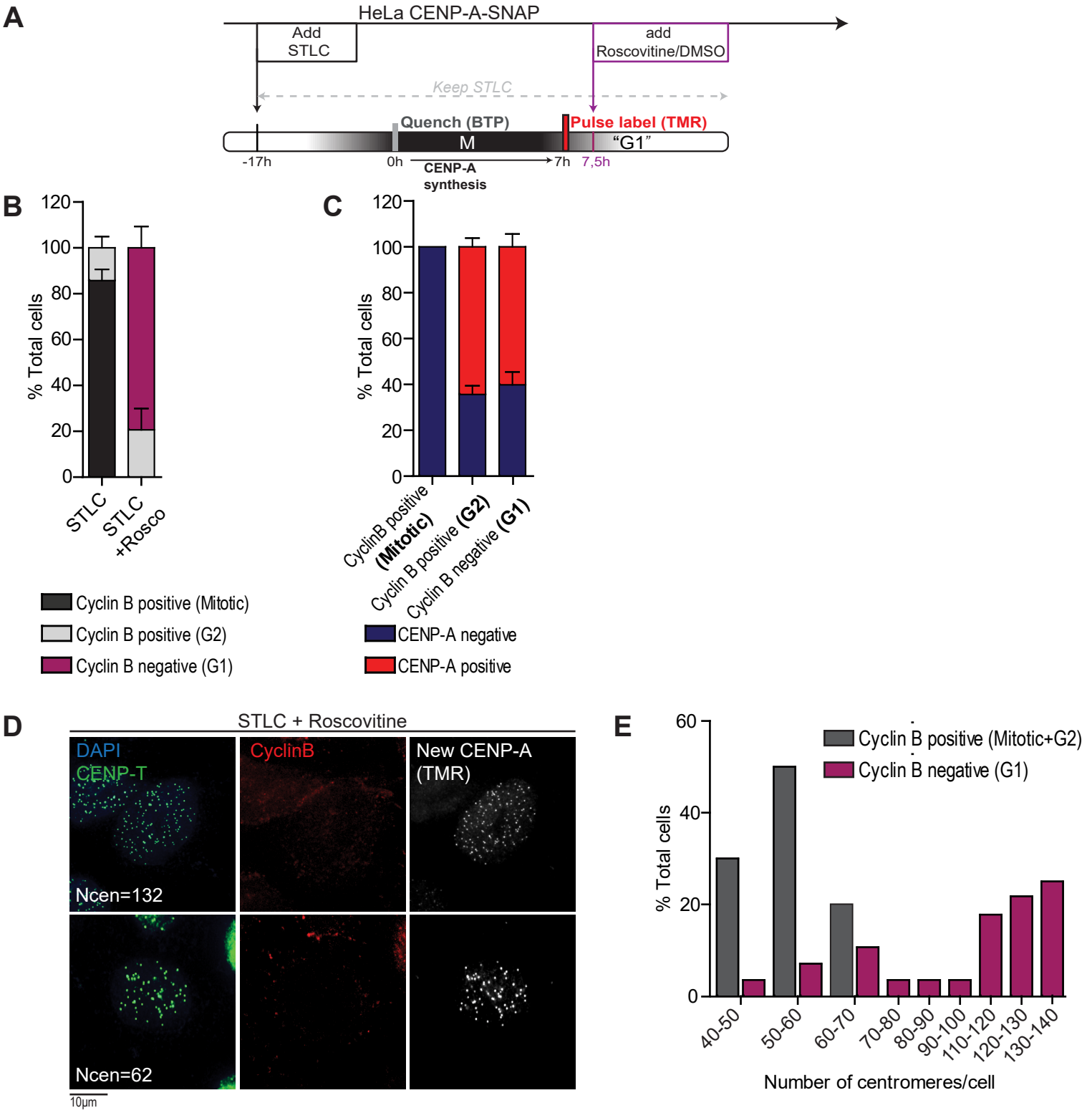
A
HeLa CENP-A-SNAP
Add STLC
add Roscovitine/DMSO
Keep STLC
Quench (BTP)
Pulse label (TMR)
M
"G1"
-17h
0h
7h
7,5h
CENP-A synthesis
B
% Total cells
STLC
STLC +Rosco
Cyclin B positive (Mitotic)
Cyclin B positive (G2)
Cyclin B negative (G1)
C
% Total cells
CyclinB positive (Mitotic)
Cyclin B positive (G2)
Cyclin B negative (G1)
CENP-A negative
CENP-A positive
D
STLC + Roscovitine
DAPI
CENP-T
CyclinB
New CENP-A (TMR)
Ncen=132
Ncen=62
10µm
E
% Total cells
Cyclin B positive (Mitotic+G2)
Cyclin B negative (G1)
40-50
50-60
60-70
70-80
80-90
90-100
110-120
120-130
130-140
Number of centromeres/cell
F
Light cells
Heavy cells
+STLC
+Roscovitine (hr)
0.5 1 2 3
+STLC
+DMSO only (hr)
0.5
H3pS10
Ponceau
G
HJURP
Ponceau

Figure S1. (supplement to Figure 1) Conditions used for SILAC analysis are permissive for CENP-A deposition.

(A) To enrich for mitotic phase, HeLa CENP-A-SNAP cells were treated with Eg5 inhibitor (STLC) for 24h. 17h into mitotic arrest, pre-existing CENP-A-SNAP pool was quenched with BTP, followed by 7h of chase. 30min before pulse labeling of newly synthesized pool of CENP-A-SNAP and fixation, cells were treated either with Roscovitine or DMSO.

(B) Quantification of frequencies of Cyclin B positive (G2 and mitotic) cells and Cyclin B negative (tetraploid cells which exited mitosis without cytokinesis due to Cdk1 inhibition, see panel D, E) in the experiment described in (A).

(C) Quantification of frequencies of CENP-A-SNAP (TMR) positive cells in each cell cycle stage present. Cells arrested in mitosis do not assemble CENP-A (left bar). Degree of CENP-A assembly in either G2 or G1 cells is assayed following Roscovitine treatment.

(D) Representative images of Roscovitine-treated cells in experiment described in (A). Cells were counterstained with Cyclin B, CENP-T and DAPI to indicate cell cycle status, centromeres and DNA respectively.

(E) Distribution of number of centromeres under experimental conditions described in (A). Doubling of centromere number indicates formation of tetraploid cells due to forced mitotic exit in the presence of STLC and Roscovitine.

(F) Western blots for the mitotic marker H3pS10 indicating cell cycle position of HeLa S3 cells used in SILAC experiment in Figure 1. Cells were arrested in mitosis with the Eg5 inhibitor STLC followed by treatment with DMSO control or Roscovitine (light cells) to force mitotic exit caused by Cdk inhibition.

(G) Western blots for HJURP (isolated from soluble fraction) from HeLaS3 cells showing dephosphorylation (as seen by shift in SDS-PAGE mobility of phosphorylated HJURP) upon Roscovitine treatment of "light" cells. Based on this, we harvested cells after 30 min of Roscovitine (or DMSO) treatment, balancing between HJURP dephosphorylation and completion of HJURP-mediated centromeric chromatin assembly.

Figure S2

A

Phospho-site(s) covered	Phosphopeptide	(Roscovitine-treated)/(Mock-treated) Ratio		
		Experiment #1 (Forward labeling)	Experiment #2 (Reverse labeling)	Experiment #3 (Reverse labeling)
HJURP pS185	VTPLPSLA**pS**PAVPAPGYCSR	**0.32**	nd	**0.30**
HJURP pS412	WLI**pS**PVK	**0.72**	nd	**0.62**
HJURP pS448	EYCL**pS**PR	**0.53**	nd	nd
HJURP pS473	GGPA**pS**PGGLQGLETR	**0.48**	**0.37**	**0.42**
HJURP pS595	**pS**PGQMTVPLCIGVSTDK	**0.23**	nd	**0.25**
	YCLK**pS**PGQMTVPLCIGVSTDK	**0.28**	nd	**0.30**
HJURP pS642	LPS**pS**PLGCR	**0.46**	**0.48**	**0.39**
CENP-A pS16+pS18	**pS**P**pS**PTPTPGPSR	nd	**0.93**	nd
	R**pS**P**pS**PTPTPGPSR	nd	**1.01**	nd
	RR**pS**P**pS**PTPTPGPSR	**0.87**	**0.98**	nd
CENP-A pS16	RR**pS**PSPTPTPGPSR	**0.94**	**1.13**	nd

nd = no data

B

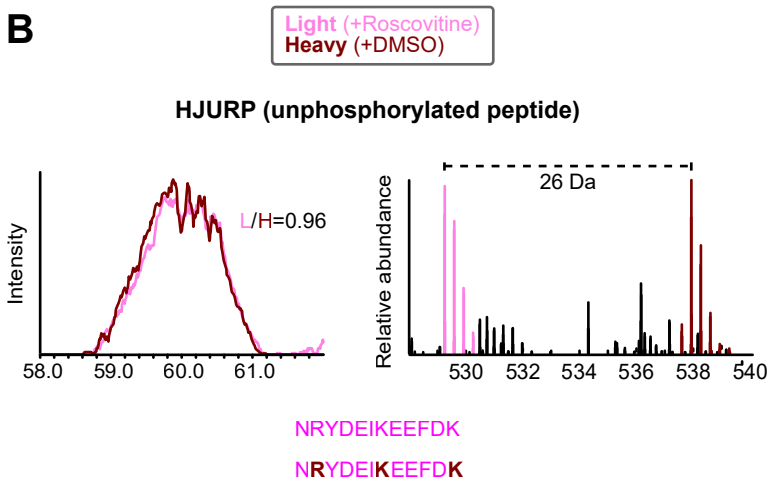

C

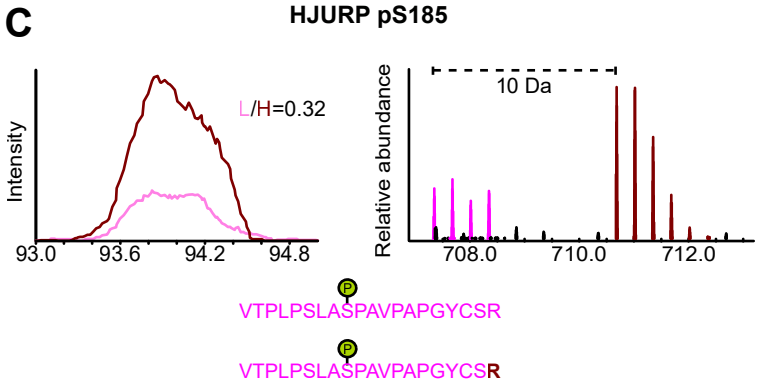

D

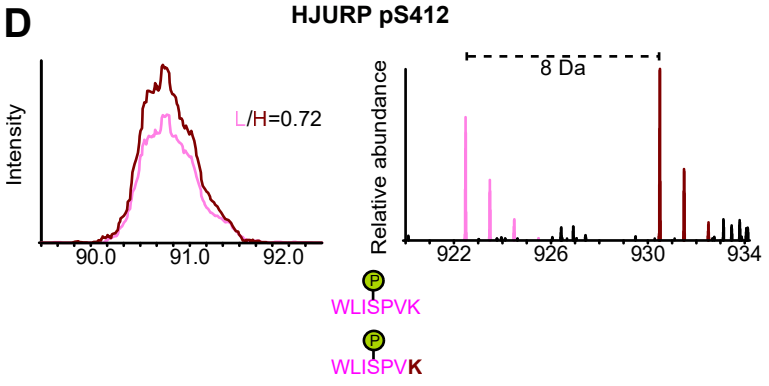

E

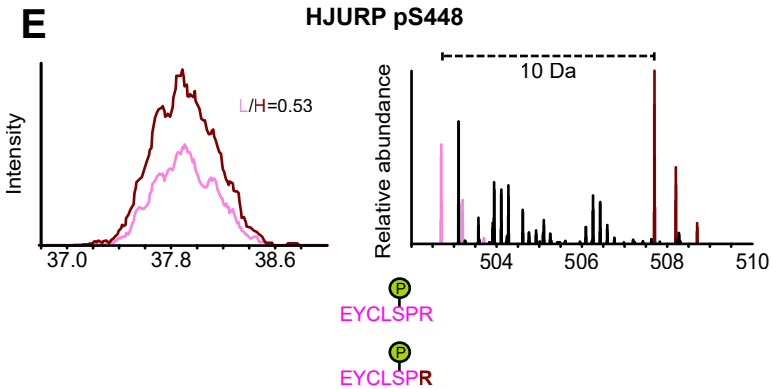

F

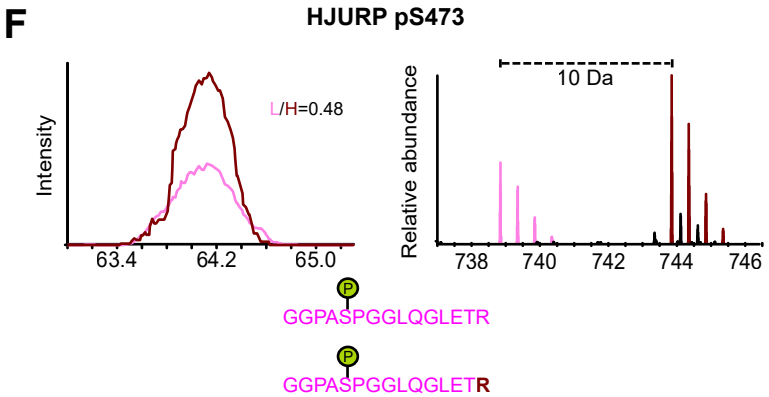

G

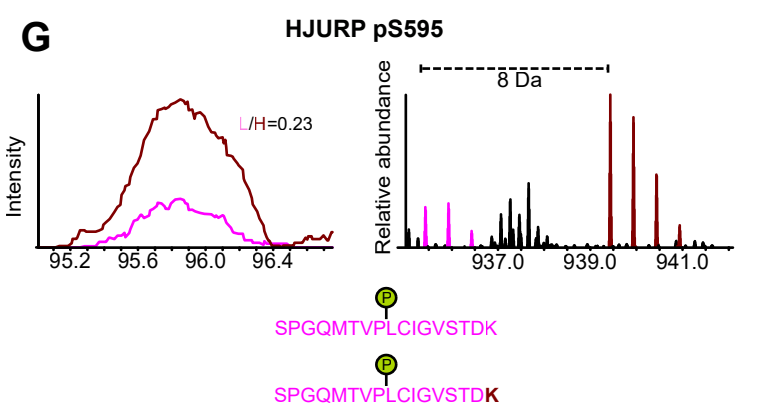

H

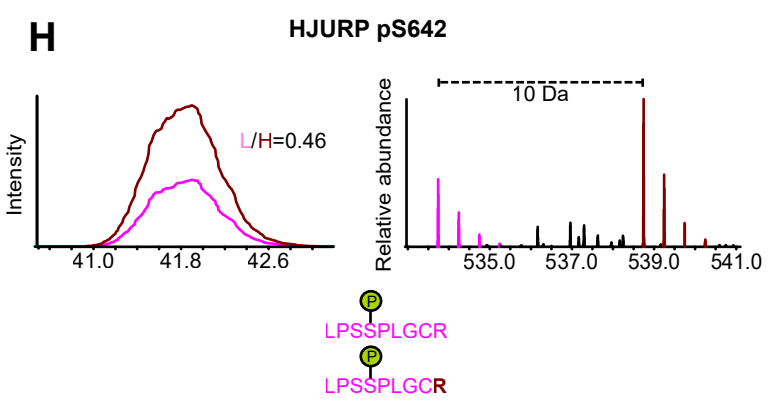

I

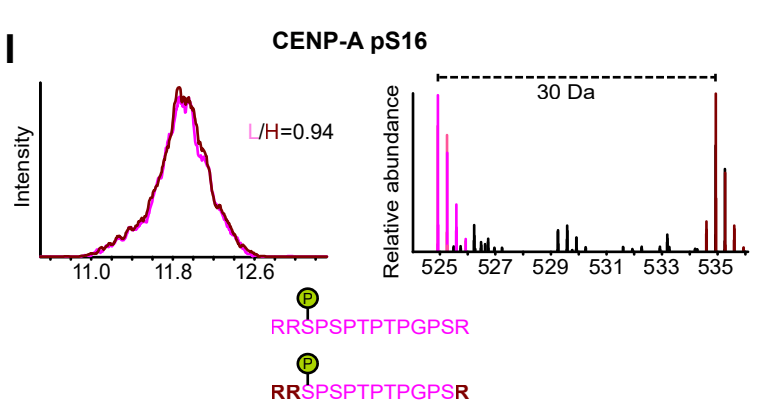

J

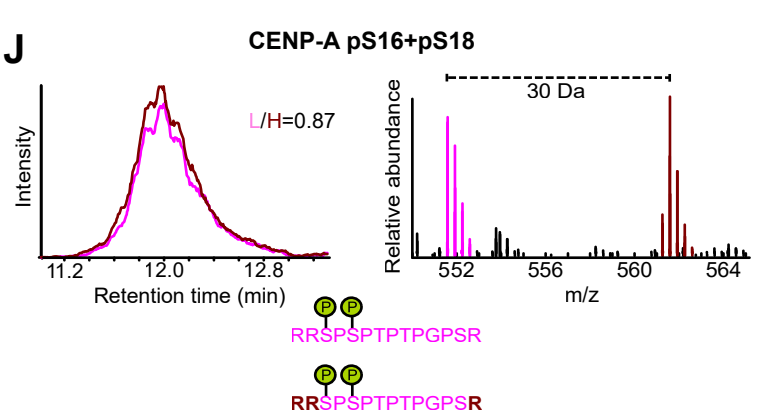

Figure S2 (supplement to Figure 1) G1/Mitotic Ratios of HJURP and CENP-A phosphopeptides are reproducible.

(A) Table summarizing data from three independent SILAC experiments (the data described in Figures 1B, are displayed in the column labeled "Experiment #1"). For the forward labeling experiment, the "light" cells are treated with Roscovitine while the "heavy" cells are mock-treated. For reverse labeling experiments, the "light" cells are mock-treated while the "heavy" cells are treated with Roscovitine. Red residues are the sites where phosphate groups were unambiguously mapped. Bolded residues are the Cdk consensus motifs in each peptide. (nd=no data).

(B-J) Representative chromatograms and spectra of HJURP and CENP-A phosphopeptides in SILAC. Extracted ion chromatograms of all phosphopeptides from Figure 1C and 1D, showing co-elution of phosphopeptide pairs (left panels), and representative mass spectra showing isotopic envelopes of light vs. heavy peptides (right panels). Phosphopeptides from "light" (Roscovitine-treated) cells are coloured in pink, while the phosphopeptides from "heavy" (mock-treated) cells are coloured in dark red. Each peptide pair is separated by a predictable mass difference (calculated from the number of lysines and arginines in the peptide), which is labeled with dotted lines between the monoisotopic peaks of light and heavy peptides.

(B) A representative unphosphorylated HJURP peptide as internal control.

(C-H) HJURP phosphopeptides.

(I-J) CENP-A phosphopeptides.

Figure S3

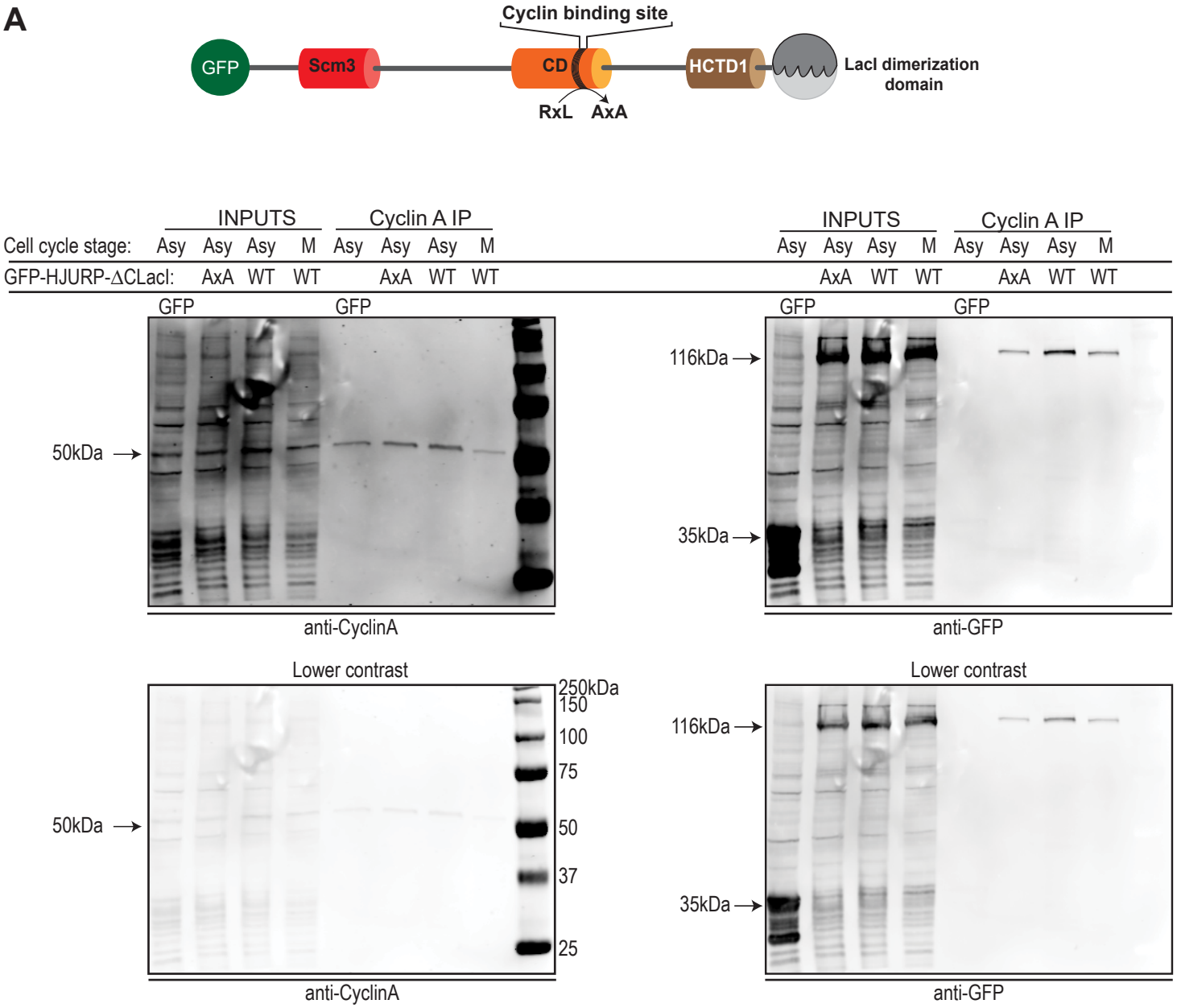
A
Cyclin binding site
GFP
Scm3
CD
HCTD1
LacI dimerization domain
RxL
AxA
INPUTS
Cyclin A IP
Cell cycle stage:
Asy Asy Asy M Asy Asy Asy M
GFP-HJURP-ΔCLacI:
AxA WT WT AxA WT WT
GFP
GFP
50kDa
116kDa
35kDa
anti-CyclinA
anti-GFP
Lower contrast
250kDa
150
100
75
50
37
25
B
INPUTS
Cyclin B IP
Cell cycle stage:
M M M M M M
GFP-HJURP-ΔCLacI:
AxA WT AxA WT
GFP AxA WT GFP AxA WT
55kDa

Figure S3. (supplement to Figure 1) Cyclin A and Cyclin B bind to HJURP.

(A) Top: Schematic of GFP-HJURP-ΔCLacI protein with relevant domains depicted. Experiments were performed with a HJURP construct in which the C-terminal homodimerization domain is replaced with that of LacI to prevent dimerization with wild type HJURP. Bottom: Raw images of a Western blot shown in Figure 1E. Upper and lower panels are identical except for different contrasting.

(B) Cyclin B interacts with HJURP in mitosis independently of Conserved Domain. Randomly cycling HEK293T cells were transiently transfected either with GFP alone, GFP-HJURP-ΔCLacI or GFP-HJURP^{AxA}-ΔCLacI. 24h post-transfection cells were treated overnight using DME III inhibitor to induce mitotic arrest. 48h post-transfection, cells were lysed and Cyclin B was immunoprecipitated using Anti-Cyclin B coated beads. Bound complexes were separated using SDS-PAGE followed by immunoblotting with indicated antibodies (raw images of Westerns are shown).

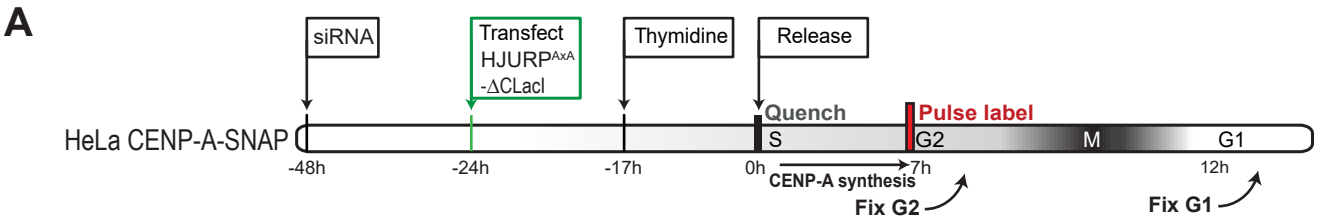
A
siRNA
Transfect HJURP^AxA -ΔCLacI
Thymidine
Release
HeLa CENP-A-SNAP
Quench
Pulse label
S
G2
M
G1
-48h
-24h
-17h
0h
7h
12h
CENP-A synthesis
Fix G2
Fix G1

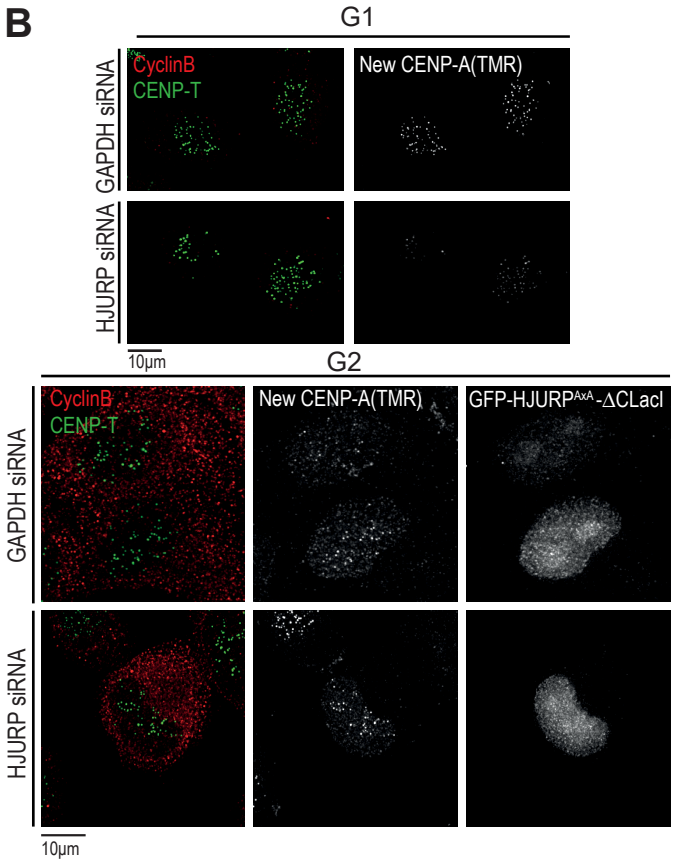
B
G1
CyclinB
CENP-T
New CENP-A(TMR)
GAPDH siRNA
HJURP siRNA
10μm
G2
GFP-HJURP^AxA-ΔCLacI

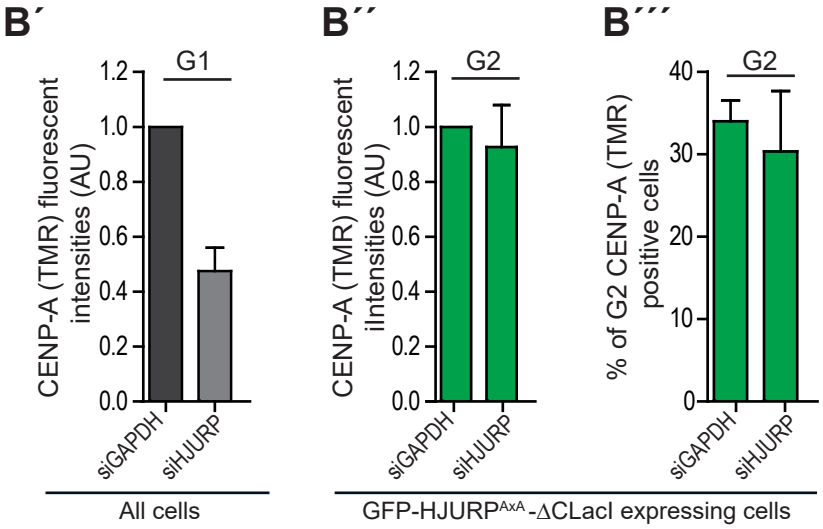
B´
B´´
B´´´
CENP-A (TMR) fluorescent intensities (AU)
% of G2 CENP-A (TMR) positive cells
siGAPDH
siHJURP
All cells
GFP-HJURP^AxA-ΔCLacI expressing cells

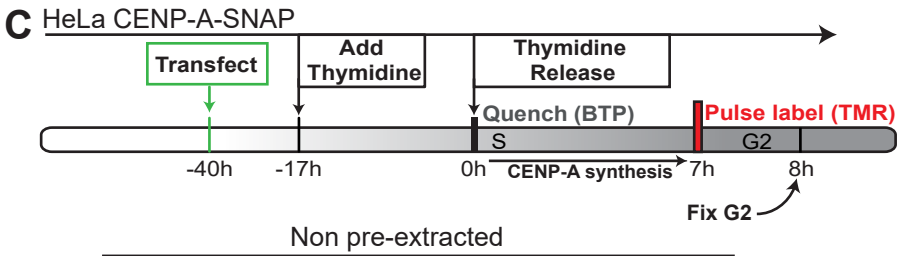
C
HeLa CENP-A-SNAP
Transfect
Add Thymidine
Thymidine Release
Quench (BTP)
Pulse label (TMR)
S
G2
-40h
-17h
0h
CENP-A synthesis
7h
8h
Fix G2

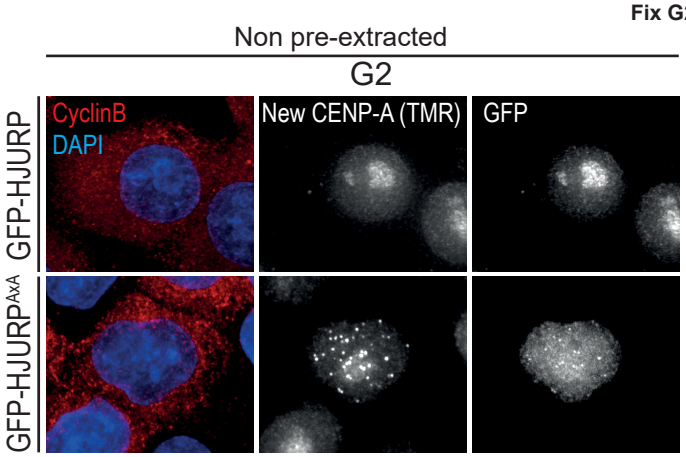
Non pre-extracted
G2
GFP-HJURP
GFP-HJURP^AxA
CyclinB
DAPI
New CENP-A (TMR)
GFP

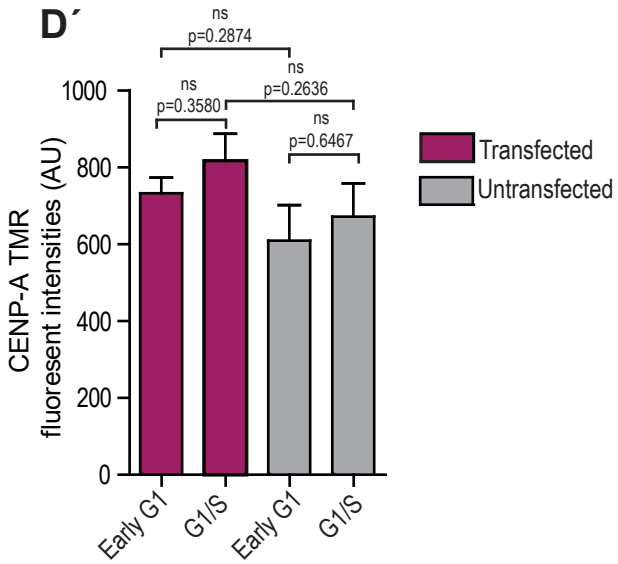
D´
CENP-A TMR fluoresent intensities (AU)
ns
p=0.2874
p=0.3580
p=0.2636
p=0.6467
Transfected
Untransfected
Early G1
G1/S

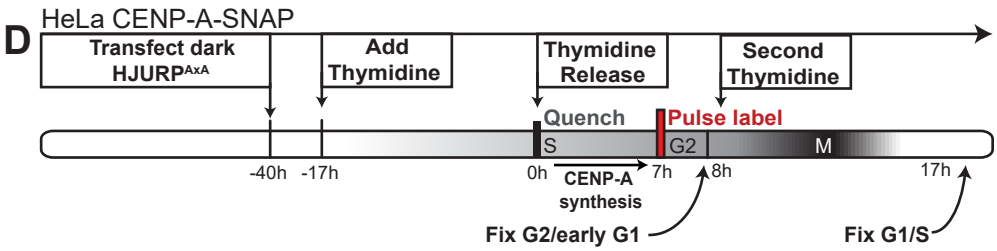
D
HeLa CENP-A-SNAP
Transfect dark HJURP^AxA
Add Thymidine
Thymidine Release
Second Thymidine
Quench
Pulse label
S
G2
M
-40h
-17h
0h
CENP-A synthesis
7h
8h
17h
Fix G2/early G1
Fix G1/S

Figure S4. (supplement to Figure 2) Centromeric targeting of HJURP and timing of CENP-A assembly is controlled by the HJURP Conserved Domain.

(A) HeLa CENP-A-SNAP cells were treated with siRNAs against HJURP or GAPDH and synchronized by double thymidine arrest and release combined with SNAP quench-chase-pulse labeling as indicated. Cells were transfected with GFP-HJURP^{AxA}-ΔCLacI 24 hours prior to synchronous release into S phase. Cells were either fixed at G2 or cycled into the next cell cycle and collected at early G1 phase, following canonical CENP-A assembly.

(B) Representative images of experiment described in (A). Cells were counterstained with Cyclin B, CENP-T and DAPI to indicate cell cycle status, centromeres and DNA respectively.

(B´) CENP-A SNAP (TMR) fluorescent signal intensities of G1 cells are plotted in grey scale. Signals are normalized to siGAPDH.

(B´´) CENP-A SNAP (TMR) fluorescent signal intensities of GFP-HJURP^{AxA}-ΔCLacI expressing G2 cells are plotted in green. Signals are normalized to siGAPDH.

(B´´´) Percentage of total G2 cell population positive for CENP-A-SNAP for indicated siRNA conditions were determined from 3 replicate experiments, plotted in green. All error bars indicate SEM.

(C) Timing of CENP-A deposition is controlled by Conserved Domain of HJURP. Experiment identical to the one described in Figure 2A, B with exception of transfection with GFP-HJURP or GFP-HJURP^{AxA}. (i.e. wild type HJURP C-terminus instead of LacI dimerization domain) Following fixation, cells are counterstained for cyclin B and DAPI to indicate G2 status, centromere localization and DNA, respectively.

(D) The apparent partiality of HJURP^{AxA}-induced G2 phase loading is not a consequence of subsequent HJURP^{AxA}-induced overloading in G1 phase to which G2 phase signals are normalized. As in Figure 2A, HeLa CENP-A-SNAP cells were either transiently transfected for 48h with untagged HJURP^{AxA} or left untransfected. 17h post-transfection cells were arrested in Thymidine for 17h followed by 7h of release, in which S phase synthesized CENP-A-SNAP was labeled by TMR. Subsequently, a set of cells were fixed (in this way, CENP-A-SNAP positive G2 and early G1 cells were obtained, as in Figure 2A, B), or Thymidine was re-added for additional 17h followed by fixation (this allowed for collection of cells arrested at G1/S phase transition). In this way, the size of pulse labeled pool of CENP-A-SNAP is identical between early G1 and G1/S arrested cells, but the time window given for CENP-A-SNAP loading is extended to the full extent of G1 phase.

(D´) Cells from the experiment described in (D) were counterstained for Cyclin B, CENP-T and Tubulin, to indicate G2 status, centromeres and the presence of a mid-body (early G1), respectively (not shown). Fluorescent (TMR) signals from all CENP-A-SNAP positive

centromeres of early G1 or G1/S cells from either condition (transfected or untransfected) were quantified using the Centromere Recognition and Quantification (CRaQ) method (Bodor et al., 2012). Error bars indicate SEM. P values are indicated on the graph (ns, Student´s t test). These results demonstrate that canonical CENP-A-SNAP loading efficiency is near its maximum in early G1 phase in HeLa CENP-A-SNAP cell line and is minimally influenced by $HJURP^{AxA}$ expression.

A

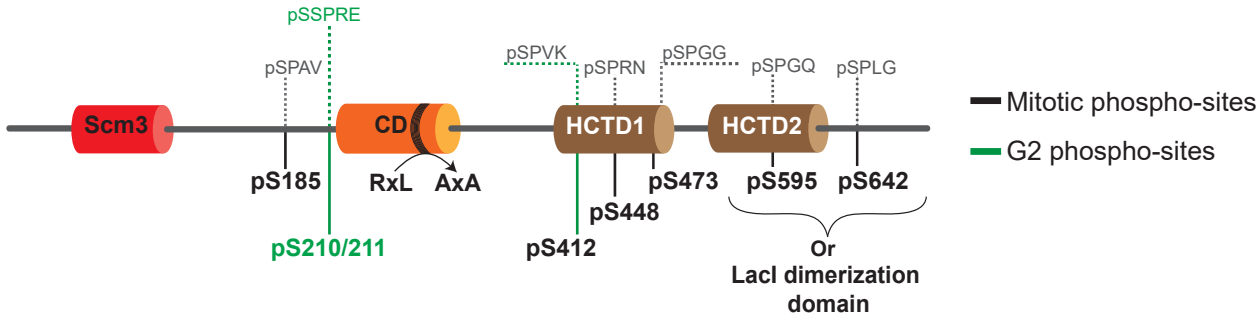

B

HJURP	**G2 phase CENP-A assembly** % intensity of G1 (% of G2 cells assembling)	
Mitotic phospho-site mutations	**C-terminal domain**	
	endogenous	**ΔC-LacI**
S185A	undetectable	undetectable
S185A, S412A, S448A,S473A	undetectable	undetectable
S595,S642A	undetectable	n.a.
S185A,S595A,S642A	undetectable	n.a.
S412,S448A,S473A	undetectable	undetectable
S185A,S412A,S448A,S473A,S595A,S642A	undetectable	n.a.
G2 phospho-site mutations		
S210A/S211A/S412A	~10% (~7%)	~10% (~15%)
S210A/S211A	undetectable	undetectable
Conserved domain mutation		
RxL>AxA	~30% (~25%)	~40% (~30%)
Other		
RxL>AxA, S412A	~30 (~50%)	n.d.

C

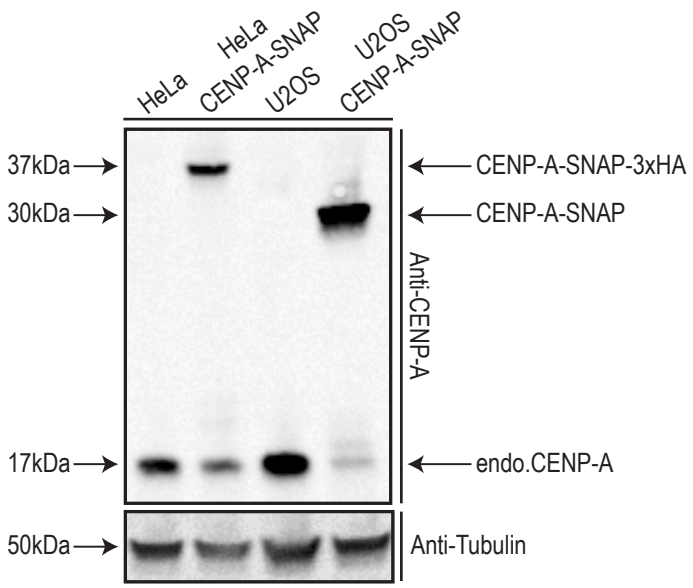

C´

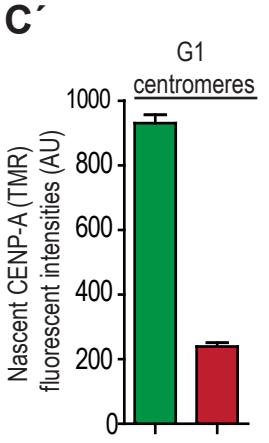

C´´

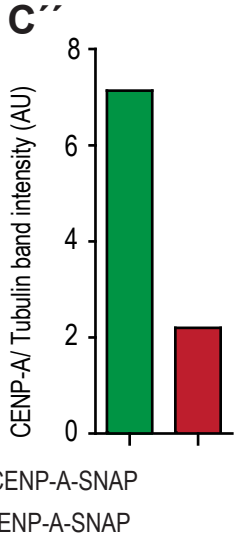

Figure S5. (**supplement to Figure 2 and 3**). **Summary of premature CENP-A assembly phenotypes of HJURP phospho-site mutants.**

(A) Schematic representation of HJURP protein, along with previously recognized domains (CENP-A binding domain (Scm3), Conserved Domain (CD), HJURP C-Terminal Domain 1 and 2 (HCTD1 and 2)) and the position of phospho-sites identified by mass spectrometry in mitosis (black lines; Figure 1, S2) or in G2 enriched cells (green lines; Figure 3). Amino acid sequences flanking phospho-sites are annotated. Position of LacI dimerization domain replacing the endogenous C-terminal dimerization domain is indicated.

(B) Table summarizing premature CENP-A assembly phenotypes upon expression of indicated mutant HJURP proteins. Experiments were performed as in Figure 2A, B. HeLa CENP-A-SNAP cells were transiently transfected with either GFP-HJURP or GFP-HJURP-ΔCLacI and congenic point mutations thereof. 23h-post transfection, cell were enriched in G2 phase by a single Thymidine block, followed by 7h of release and subsequent fixation. CENP-A assembly was assayed using SNAP TMR-labeling of its S phase synthesized pool. Following fixation, cells were counterstained for cyclin B and DAPI to indicate G2 status and DNA, respectively. Efficiency of CENP-A assembly is indicated as % of G1 phase CENP-A intensities and % of transfected cells loading. undetectable: no centromere signals were discernable. n.d. not determined. n.a. not applicable.

(C) Western blot showing higher levels of CENP-A-SNAP transgene in U2OS cell line (Müller et al., 2014) compared to HeLa cell line (used in this study). Extracts of randomly cycling U2OS CENP-A-SNAP and HeLa CENP-A-SNAP cell lines together with respective parental cell lines (carrying no transgene) were separated by SDS-PAGE followed by immunoblotting with anti-CENP-A and anti-Tubulin antibodies.

(C´) Quantification of CENP-A-SNAP band intensities of Western blot showed in (C) using Odyssey infrared scanner. Band intensities of CENP-A-SNAP were normalized to tubulin (loading control).

(C´´) Quantification of G1 CENP-A-SNAP fluorescent intensities from HeLa CENP-A-SNAP and U2OS CENP-A-SNAP. Randomly cycling HeLa CENP-A-SNAP and U2OS CENP-A-SNAP were subjected to Quench-Chase-Pulse experiment (as in Figure 2A, B). CENP-A-SNAP (TMR) fluorescent signal intensities were determined using CRaQ method.

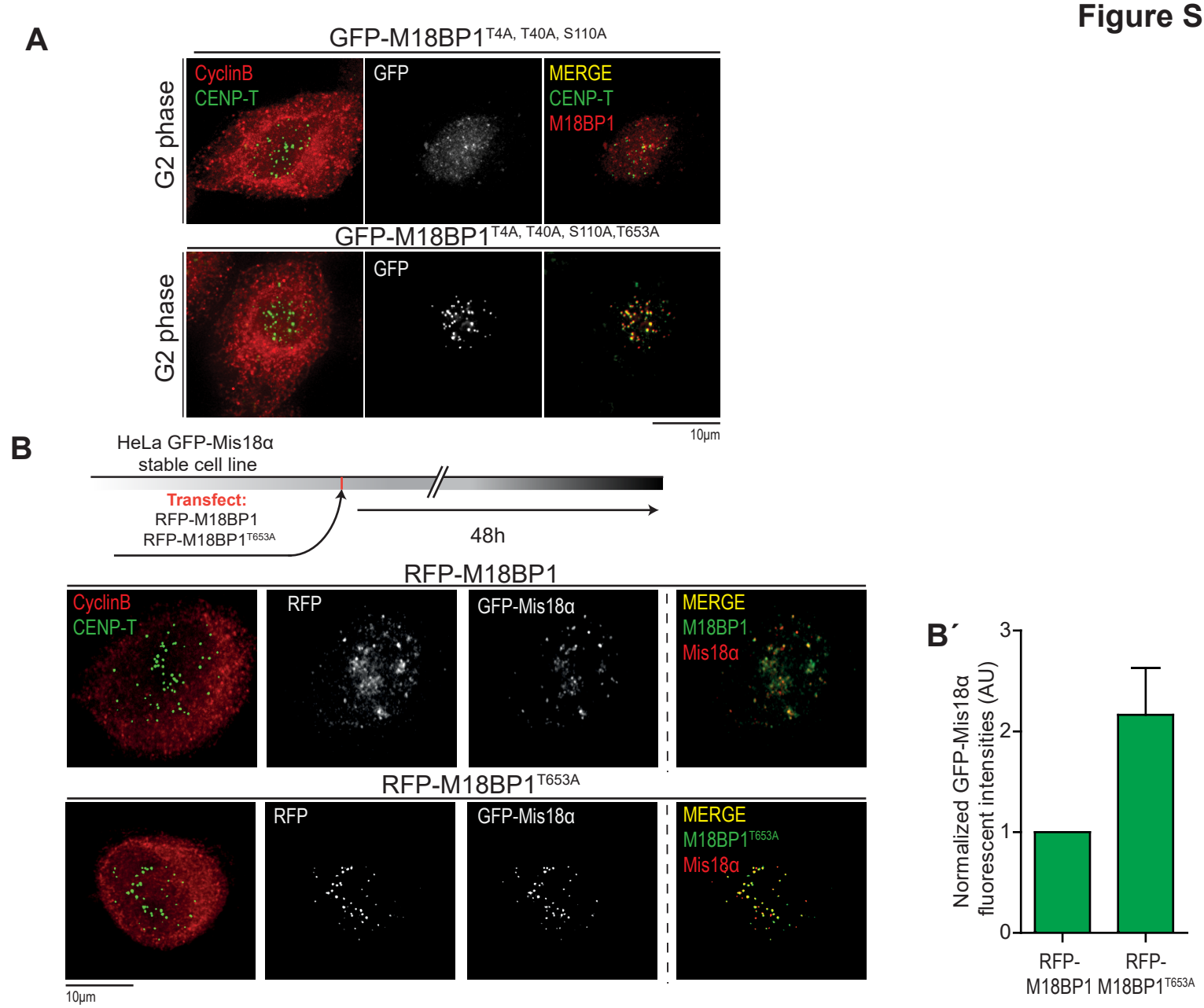
A
GFP-M18BP1T4A, T40A, S110A
G2 phase
CyclinB
CENP-T
GFP
MERGE
CENP-T
M18BP1
GFP-M18BP1T4A, T40A, S110A,T653A
G2 phase
GFP
10μm
B
HeLa GFP-Mis18α
stable cell line
Transfect:
RFP-M18BP1
RFP-M18BP1T653A
48h
RFP-M18BP1
CyclinB
CENP-T
RFP
GFP-Mis18α
MERGE
M18BP1
Mis18α
RFP-M18BP1T653A
RFP
GFP-Mis18α
MERGE
M18BP1T653A
Mis18α
10μm
B´
Normalized GFP-Mis18α fluorescent intensities (AU)
0
1
2
3
RFP-M18BP1
RFP-M18BP1T653A
C
HeLa GFP-Mis18α
stable cell line
Transfect:
RFP-M18BP1
CBdb-RFP-M18BP1
CBdb-RFP-M18BP1T653D
48h
G2
CyclinB
CENP-T
RFP-M18BP1
GFP-Mis18α
CBdbd-RFP-M18BP1
CBdbd-RFP-M18BP1T653D
M
DAPI
CENP-T
CBdbd-RFP-M18BP1
GFP-Mis18α
10μm
M18BP1
RFP
CENP-B DNA binding domain (CBdbd)
H3 nucleosomes
CENP-A nucleosomes
Alphoid DNA

Figure S6. (supplement to Figure 5) Cell cycle control of M18BP1/Mis18α complex formation

(A) M18BP1^{T4,T40,S110} triple mutant is enriched at G2 centromeres, whereas M18BP1^{T4,T40,S110,T653A} quadruple mutant is strongly enriched at G2 centromeres. Constructs expressing M18BP1^{T4,T40,S110} or M18BP1^{T4,T40,S110,T653A} were transfected into asynchronous HeLa cells 48hr prior to fixation, followed by counterstaining for cyclin B, CENP-T and DAPI to indicate G2 status, centromeres and DNA, respectively.

(B) T653 residue in M18BP1 does not determine Mis18 complex formation. Left: Asynchronously cycling HeLa cells stably expressing GFP-Mis18α were transfected with constructs expressing RFP-M18BP1 or RFP-M18BP1^{T653A} 48hr prior to fixation, followed by counterstaining for cyclin B and CENP-T to indicate G2 status and centromeres respectively. Right: Average centromeric GFP fluorescent signals from Cyclin B positive cells were determined from 3 replicate experiments. Intensities were normalized to GFP-M18BP1. Error bars indicate standard error of the mean (SEM).

(C) M18BP1/Mis18α complex formation is not inhibited by Cdk activity in G2 phase. Asynchronously cycling HeLa cells stably expressing GFP-Mis18α were transfected with constructs expressing RFP-M18BP1, CBdbd-RFP-M18BP1 or CBdbd-RFP-M18BP1^{T653D} 48hr prior to fixation, followed by counterstaining for cyclin B and CENP-T to indicate G2 status and centromeres respectively. To enrich for mitotic stages, cells were treated with Nocodozole for 5h.

Figure S7

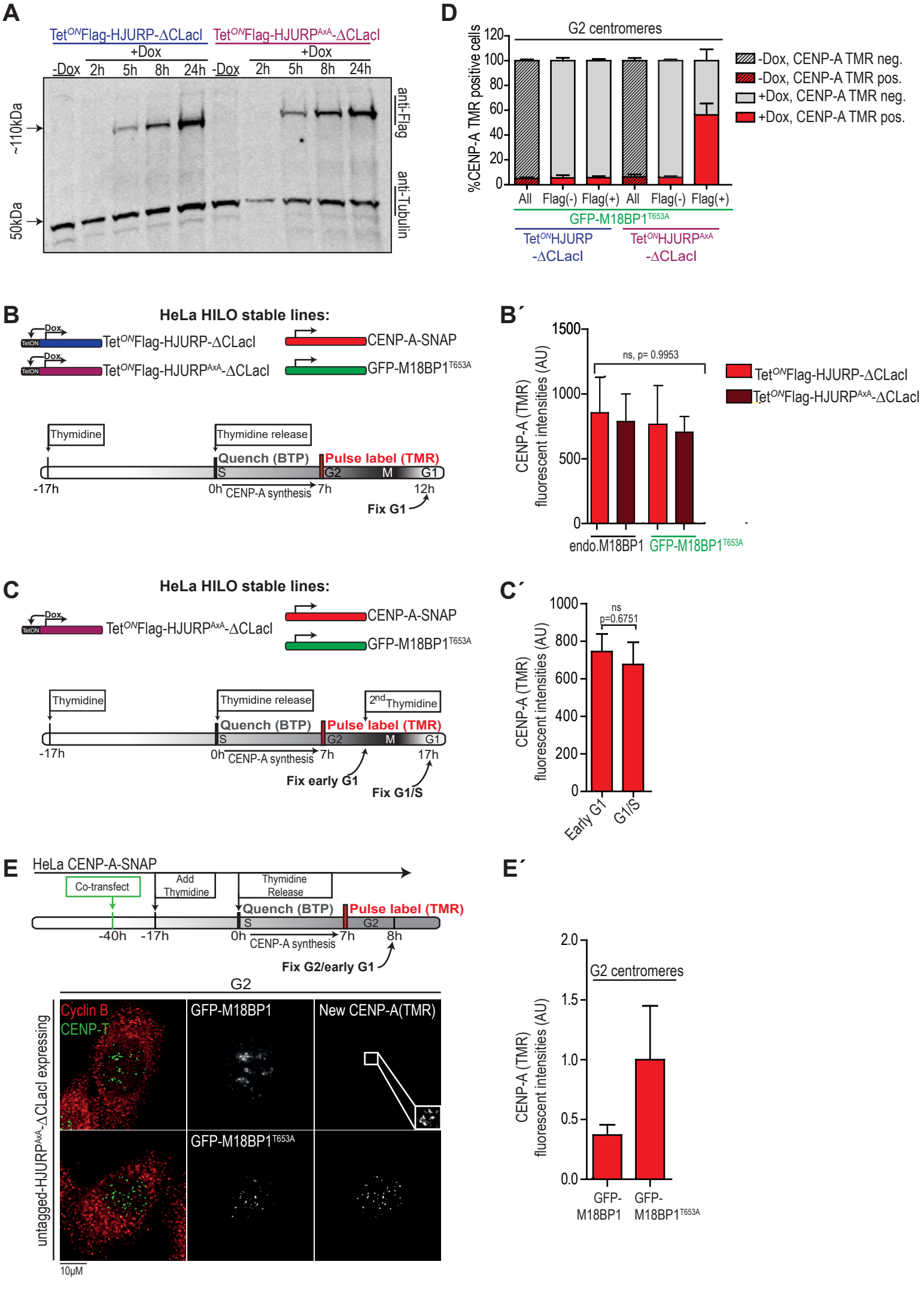
A
TetON Flag-HJURP-ΔCLacI
TetON Flag-HJURPAxA-ΔCLacI
+Dox
-Dox 2h 5h 8h 24h -Dox 2h 5h 8h 24h
~110kDa
50kDa
anti-Flag
anti-Tubulin
D
G2 centromeres
%CENP-A TMR positive cells
-Dox, CENP-A TMR neg.
-Dox, CENP-A TMR pos.
+Dox, CENP-A TMR neg.
+Dox, CENP-A TMR pos.
All Flag(-) Flag(+) All Flag(-) Flag(+)
GFP-M18BP1T653A
TetONHJURP -ΔCLacI
TetONHJURPAxA -ΔCLacI
B
HeLa HILO stable lines:
Dox
TetON
TetONFlag-HJURP-ΔCLacI
TetONFlag-HJURPAxA-ΔCLacI
CENP-A-SNAP
GFP-M18BP1T653A
Thymidine
Thymidine release
Quench (BTP)
Pulse label (TMR)
S G2 M G1
-17h 0h CENP-A synthesis 7h 12h
Fix G1
B´
CENP-A (TMR) fluorescent intensities (AU)
ns, p= 0.9953
endo.M18BP1 GFP-M18BP1T653A
C
HeLa HILO stable lines:
2nd Thymidine
-17h 0h CENP-A synthesis 7h 17h
Fix early G1
Fix G1/S
C´
ns
p=0.6751
Early G1 G1/S
E
HeLa CENP-A-SNAP
Co-transfect
Add Thymidine
Thymidine Release
-40h -17h 0h CENP-A synthesis 7h 8h
Fix G2/early G1
G2
untagged-HJURPAxA-ΔCLacI expressing
Cyclin B
CENP-T
GFP-M18BP1
New CENP-A(TMR)
GFP-M18BP1T653A
10μM
E´
G2 centromeres
GFP-M18BP1
GFP-M18BP1T653A

Figure S7. (supplement to Figure 6) Characterization of HeLa HILO inducible HJURP cell lines and CENP-A assembly dynamics.

(A) 3xFlag-HJURP-ΔCLacI and 3xFlag-HJURP^{AxA}-ΔCLacI proteins are induced to a similar extent. HeLa HILO CENP-A-SNAP, GFP-M18BP1^{T653A} carrying tetracycline-inducible 3xFlag-HJURP-ΔCLacI or3xFlag-HJURP^{AxA}-ΔCLacI were synchronized by a single Thymidine block, and released into G2 phase. Doxycycline (Dox) was added for 2h, 5h, 8h or 24h. Following fixation, whole cell lysates were separated using SDS-PAGE followed by immunoblotting with indicated antibodies.

(B) CENP-A-SNAP loading efficiency in G1 is equal in all HeLa HILO cell lines used in this study. Overview of HILO transgenes are shown. Uninduced HeLa HILO CENP-A-SNAP cells carrying indicated M18BP1 and or HJURP transgenes were synchronized by addition of Thymidine for 17h, followed by a release for 7h during which a nascent CENP-A-SNAP pool was fluorescently labeled. Cells were allowed to cycle into early G1 phase, 12h post release and fixed (early G1 as in Figure 6). This experimental set-up allows for labeling of an equal pool of nascent CENP-A-SNAP and compares the degree of assembly across cell lines used (conditions analogous to the ones in Figure 6).

(B´) CENP-A-SNAP fluorescent intensities were quantified using CRaQ method and tested for statistically significant differences (ns, one-way ANOVA). Results indicate that G1 phase levels are similar across all cell lines used. Error bars indicate SEM.

(C) CENP-A loading in G1 in 3xFlag-HJURP^{AxA}-ΔCLacI / GFP-M18BP1^{T653A} expressing cells as near its maximum in early G1 phase. Relevant transgenes are shown. Experimental condition is identical to (B) except that in addition to fixation in early G1 phase, a subset of cells were allowed to cycle through G1 and were collected at the G1/S boundary following a second Thymidine addition.

(C´) CENP-A-SNAP fluorescent intensities from early G1 cells and cells collected at the end of G1 were directly compared and tested for statistically significant differences (ns, one-way ANOVA). Results indicate that early and late G1 phase levels are similar. CENP-A-SNAP fluorescent intensities were quantified using CRaQ method. Error bars indicate SEM. P values are indicated on the graph (ns, Student´s t test).

(D) Fraction of cells assembling CENP-A upon mutant M18BP1 and/or mutant HJURP expression. Data from experiment shown in Figure 6. Here the frequency of CENP-A-SNAP G2 centromeres is plotted as a fraction of total Flag positive cells, except for un-induced samples, in which the fraction of total cells was determined. Averages of 3 independent experiments are shown. Error bars indicate SEM.

(E) Over-expression of GFP-M18BP1 does not enhance HJURP^{AxA}-driven precocious CENP-A deposition. HeLa CENP-A-SNAP cells were enriched in G2 phase by a single Thymidine arrest, followed by 7 h release. 40 h prior to synchronized S phase release, cells were co-transfected with untagged-HJURP^{AxA}-ΔCLacI combined with either GFP-M18BP1 or GFP-M18BP1^{T653A}. S phase synthesized CENP-A-SNAP was pulse labeled in G2 phase to assay CENP-A assembly. Cells were counterstained for cyclin B and CENP-T to indicate G2 status and centromeres, respectively.

(E´) Quantification of CENP-A-SNAP (TMR) fluorescent signal intensities of experiment in A. Average centromeric CENP-A-SNAP fluorescent signals from G2 cells (Cyclin B positive) and G1 cells (Cyclin B negative) were determined from 4 replicate experiments using CRaQ method. Signal intensities were normalized to CENP-A-SNAP in G1 cells expressing GFP-M18BP1. Error bars indicate SEM. GFP-M18BP1 force expression in combination with HJURP^{AxA}-ΔCLacI results in similar of CENP-A assembly as in the presence of endogenous M18BP1 levels (see also Figure 2B, B´)

Supplemental Experimental Procedures

DNA constructs

HJURP-GFP (pLJ381) and GFP-HJURP-ΔCLacI (pLJ632) (Zasadzińska et al., 2013), in which amino acids 483-743 (C-terminus) were replaced by dimerization domain of LacI (Zasadzińska et al., 2013) were a gift from Dan Foltz (Northwestern University of Chicago). GFP-HJURP (pLJ380) and GFP-HJURP-ΔCLacI (pLJ632) were converted to GFP-HJURP^{AxA} (pLJ600) and GFP-HJURP^{AxA}-ΔCLacI (pLJ654) by quick exchange PCR replacing R276 and L278 by Alanine. GFP-HJURP$^{S210A, S211A, S412A}$ (pLJ828) or GFP-HJURP$^{S210A, S211A, S412A}$-ΔCLacI (pLJ830) was made via quick exchange PCR. pLJ591, HJURP-CBdbd-GFP was created by PCR amplification of the first 158 N-terminal amino acids of CENP-B protein [CENP-B DNA binding domain (CBdbd)] and ligation to the N terminus of pLJ383 (a GFP-Mis18α construct). Subsequently, Mis18α was excised using EcoRI/BamHI restriction, followed by T4 end blunting and ligation, resulting in CBdbd-GFP vector. The CBdbd fragment was subsequently inserted in frame in between HJURP and GFP of pLJ381. For the creation of the HeLa HILO 3xFlag-HJURP-ΔCLacI /HJURP^{AxA}-ΔCLacI inducible cell lines, the donor plasmid pRD-RIPE (Khandelia et al., 2011) was digested with AgeI and BsrGI to remove EGFP followed by insertion of the LacI dimerization domain. Next, PCR amplified 3xFlag-HJURP-ΔC (aa 1-482) or 3xFlag HJURP^{AxA}-ΔC (aa 1-482) was inserted into an AvaI/BsrGI digested vector, resulting in an in-frame fusion of 3xFlag HJURP/HJURP^{AxA}-ΔCLacI (designated pLJ745 and pLJ746, respectively). GFP-M18BP1^{T653A} (pLJ649) was created by quick exchange PCR using GFP-M18BP1 as a template (pLJ415 (Silva et al., 2012)). An analogous procedure was employed to generate GFP-M18BP1^{T653D} (pLJ699). CBdbd-GFP-M18BP1 (pLJ592) was generated by ligation of CBdbd fragment between GFP and M18BP1 of the GFP-M18BP1 plasmid (pLJ415) mRFP-M18BP1^{T653D} (pLJ705) was created by NotI and AfeI replacement of GFP with mRFP (from pLJ287). CBdbd-mRFP-M18BP1/M18BP1^{T653D}/M18BP1^{T653E} (pLJ697, pLJ700 and pLJ642, respectively) were created by PCR insertion of CBdbd fragment from pLJ591 (CBdbd-GFP-HJURP) into pLJ534 (mRFP-M18BP1) or pLJ705 (mRFP-M18BP1^{T653D}) or pLJ641 (mRFP-M18BP1^{T653E}). PCR amplified CBdbd was subsequently fused to N-terminal portion of mRFP. All plasmid inserts were verified by DNA sequencing.

Cell lines and culturing conditions

All human cell lines used were grown at 37°C, 5% CO_2. Cells were grown in DMEM (Bio West) supplemented with 10% fetal bovine serum (FBS) (BioWest)), 2 mM glutamine, 1 mM sodium pyruvate (SP) (Thermo Fischer Scientific), 100 U/ml penicillin, and 100 µg/ml streptomycin, with the exception of HeLa HILO derived cell lines in which 10% tet-free (BioWest) FBS was used. HeLa HILO RMCE cell lines were a gift from E.V. Makeyev, Nanyang Technological University, Singapore, and contain a single genomic recombination

which allows for the insertion of a tetracycline responsive expression cassette (Khandelia et al., 2011). The four lines outlined in Figure 6 were assembled as follows: HeLa HILO RMCE clone #10 (Khandelia et al., 2011), was transfected with (pLJ649) that constitutively drives GFP-M18BP1^{T653A} expression. Positive clones were selected with 500 µg/ml of Neomycin (Gibco). A polyclonal population was sorted based on GFP fluorescence. A single clone of HeLa HILO GFP-M18BP1^{T653A} as well as the parental HILO RMCE clone #10 were transduced with pBABE-CENP-A-SNAP-3xHA retrovirus (pLJ718) (Bodor et al., 2012). Infected cells were selected by 300 µg/ml of Hygromycine (Invitrogen). Individual resistant cells were sorted by FACS. CENP-A-SNAP-3xHA clones #9 and #10, respectively were selected for further analysis. This selection was based on equal expression of CENP-A-SNAP-3xHA between different cell lines, as determined by immunoblot using rabbit anti-CENP-A (Cell Signaling technology) and by TMR fluorescent intensities. Both clones were then transfected with 2,5 ng/µl of pLJ745 and pLJ746, vectors carrying two loxP sites flanking the Doxycycline (Dox) inducible 3xFlag-HJURP or 3xFlag-HJURP^{AxA} expression construct. Cre recombinase (Khandelia et al., 2011) was added at 1% of total DNA content. Positive clones were selected using 1 µg/ml of Puromycin (MERCK). Expression of 3xFlag-HJURP/HJURP$^{WT/AxA}$ was induced by 10 µg/ml of Doxycycline (Sigma-Aldrich) and assayed for equal expression by western blot using FlagM2 antibody (Sigma-Aldrich). U2OS CENP-A-SNAP cell lines were gift from Genevieve Almouzni (Institut Curie, France).

DNA transfection and siRNA treatment

Transient transfection of HeLa CENP-A-SNAP and HEK293T was performed using Lipofectamine LTX (Invitrogen; Carlsbad, CA) according to the manufacturer's instructions. All siRNAs were obtained from Dharmacon. Mis18α and HJURP were depleted as previously reported (Silva et al., 2012; Zasadzińska et al., 2013, respectively).

Co-Immunoprecipitation

HEK293T cells were transiently transfected either with GFP alone, GFP-HJURP-ΔCLacI or GFP-HJURP^{AxA}-ΔCLacI. 24h post-transfection cells were either allowed to continue to cycle or were treated overnight in DME III to induce mitotic arrest. 48h post-transfection, 10^7 cells were harvested in ice-cold PBS for 5 min at 3,200 x g and lysed in buffer containing 3,75mM Tris pH 7,5, 20mM KCl,0,5mM EDTA, 0,1% digitonin and 0,4 µM DTT. Lysates were homogenized using a 27G needle, and spun at 300 x g for 5 min. This was repeated two times, followed by combining two supernatants and spin clarification at 10,000 x g for 15 min. Soluble fraction was collected and KCl concentration was adjusted to 150 mM. 5µg/ml of anti-Cyclin A coated agarose beads (Santa Cruz Biotechnology) or anti-Cyclin B (Santa Cruz Biotechnology) was equilibrated in lysis buffer prior to pulldown. After immunoprecipitation, beads were washed once in wash buffer A (20mM HEPES, 20Mm M KCl, 0,4m M DTT and 0,4mM EDTA) and two times in wash buffer B (wash buffer A with

225mM NaCl for Cyclin A pulldown, and 150mM NaCl for Cyclin B). Complexes bound to the beads were eluted using 2% SDS for 20 min, followed by immunoblotting with anti-Cyclin A (Santa Cruz) (Figure 1E) or anti-Cyclin B (Santa Cruz) (Figure S3B) and anti-GFP (Chromotek) antibodies. IRDye800CW-coupled anti-rat (Licor Biosciences) and DyLight680-coupled anti-rabbit (Rockland Immunochemicals, Gilbertsville, PA) secondary antibodies were used prior to detection on an Odyssey near-infrared scanner (Licor Biosciences, Lincoln, NE). Immunoblot signals were quantified using the Odyssey software (see also (Bodor et al., 2014)). GFP signal values were normalized to their respective Cyclin A signals and to corresponding GFP input values.

SILAC and affinity purification of prenucleosomal HJURP/CENP-A/H4 complex

SILAC labeling medium (MEM Eagle Joklik Modification) deficient in lysine and arginine was reconstituted according to manufacturer's instructions (Sigma-Aldrich), and supplemented with normal lysine and arginine (Sigma-Aldrich) for "light" medium, and 50 mg/ L $^{13}C_6$,$^{15}N_2$-lysine and 50 mg/L $^{13}C_6$, $^{15}N_4$-arginine (Silantes) for "heavy" medium. Both media were supplemented with 10% dialyzed FBS (Gemini), GlutaMax (Gibco), 1 mM HEPES, 1% Pen/Strep, MEM non-essential amino acids (Gibco), and 120 mg/L proline to prevent arginine-to-proline conversion. Two parallel cultures of previously characterized HeLaS3 cells stably expressing localization and purification (LAP)-tagged CENP-A (Bailey et al., 2013) were cultured in spinner flasks for at least 6 cell doublings to allow full incorporation of the stable isotope-containing amino acids. Heavy isotope labeling efficiency of ~98% was confirmed by mass spectrometry after trypsin digestion of proteins extracted from heavy-labeled cells. To enrich for mitotic cells, both cultures were treated with 50 μM S-trityl-L-cysteine for 17 h. Subsequently, the "light" cells were treated with 100 μM R-Roscovitine (AdipoGen) for 30 min while the "heavy" cells were mock-treated with DMSO. Cell cycle status and HJURP phospho-status was monitored by immunoblotting for H3pS10 (Upstate) and an anti-HJURP antibody generated against a C-terminal fragment (1 μg/ml) (Bassett et al., 2012, Dev Cell), respectively. Cell pellets from 1.4 x 10^9 of "light" and "heavy" cells were combined in 1:1 ratio. Affinity purification of the prenucleosomal HJURP/CENP-A/H4 complex was performed as previously described (Bailey et al., 2013) except that protein elution was performed with 2% SDS and heating at 95°C.

Mass spectrometry and data analysis

Purified CENP-A and associated proteins were precipitated using pre-chilled acetone (4 X volume) followed by successive washing. Dried protein pellets were reconstituted with 0.1% RapiGest SF Surfactant (Waters) in 100 mM NH_4HCO_3, pH 8.0. Resuspended proteins were reduced using DTT, alkylated with iodoacetamide, and digested using trypsin. Since trypsin cleaves only after lysines and arginines, this ensures that every resulting peptide will contain at least one lysine or arginine, so that all heavy peptides are distinguishable

from their corresponding light peptides by predictable mass differences. Rapidgest was removed by adding 0.5% TFA and incubation for 30min at 37°C. The peptides were desalted with StageTips (Rappsilber et al., 2007), followed by phosphopeptide enrichment by TiO2 prior to analysis by Q-Exactive Hybrid Quadrupole-Orbitrap mass spectrometer (Thermo Fisher Scientific). The pFind search engine was used to search the UniProt human protein database to identify peptides (Wang et al., 2007). Quantification was done using extracted-ion chromatograms (XICs) of each light and heavy peptide pair, and L/H ratio represents the ratio of total area under each elution peak. Mass spectra of a representative non-phosphorylated HJURP peptide from the flow through in Figure 3 of samples from cells containing HJURP and HJURP^{AxA} had a retention time range of 28.75-29.89min, which includes all scans in both runs in which the peptide was detectable. Mass spectra of the phosphopeptide containing pS210/pS11, from the elution of the phospho-enrichment from cells containing HJURP and HJURP^{AxA} had a retention time range of 24.00-25.48min, which includes all scans from both runs in which the peptide was detectable.

Phospho-specific anybody generation, application and phosphatase treatment

Phospho-specific rabbit antibody for M18BP1 was produced by immunization of 2 rabbits with phosphorylated peptide ((NH2-)CKAYILV (pT)PLKSRK (-CONH2)), and subsequent affinity purification of both sera (Innovagen AB, SE-22370 Lund, Sweden). 10^6 of transiently transfected HEK293T carrying either GFP M18BP1 or GFP M18BP1^{T653A} were lysed in buffer containing 75mM HEPES pH 7,5, 150mM NaCl, 2mM MgCl2, 0,1% NP-40, 5% Glycerol, 2mM EDTA supplemented with Roche complete protease and phosphatase inhibitors. Lysates were spun at 4°C for 5 min at 15,000 x g. Supernatants were either left untreated or 300 units of Lambda phosphatase was added. All samples were incubated for 30 min at 30°C. Reaction was stopped by addition of 4 x Orange sample buffer. For assaying Cdk dependent phosphorylation of M18BP1, transiently transfected Hek293T were treated with 100μM of Roscovitine for 30min, or treated for DMSO. Protein extracts were separated by SDS-PAGE and probed with pT653 and GFP (Chromotek) antibodies. Fluorescence activated cell sorting (FACS) for cell cycle profile was performed based on propidium iodide staining as described (Silva et al., 2012).

Immunofluorescence and pre-extraction procedure

Procedures are essentially as described (Bodor et al., 2012). Briefly, all cell lines were grown on glass coverslips coated with poly-L lysine (Sigma-Aldrich) and fixed with 4% formaldehyde (Thermo Scientific) for 10 min followed by permeabilization in 0.1% Triton X-100. HeLa cells were stained with anti-cyclin B1 (1:50; sc-245, Santa Cruz) and anti-CENP-T (Barnhart et al., 2011). Secondary antibodies used were either FITC-conjugated anti-mouse (Jackson Immunoresearch Laboratories) or Dy680 conjugated anti-rabbit antibody (Rockland Immunochemicals). Cells were stained with DAPI (40, 6-diamidino-2-

phenylindole; Sigma-Aldrich) before mounting in Mowiol. For detecting GFP HJURP^{AxA} on G2 centromeres, HeLa CENP-A SNAP cells transiently expressing the construct were pre-extracted for 5min using CSK buffer (10mM Pipes-KOH pH7, 100mM NaCL, 300mM Sucrose and 3mM $MgCl_2$) supplemented with 0.3% of Titon X-100. Subsequently, cells were washed one time with CSK buffer, followed by PBS wash and fixation for 22 min with 4% formaldehyde. Cells were counterstained using anti-CENP-T (Barnhart et al., 2011) and anti-Aurora B (1:100; BD transduction laboratories). GFP HJURP^{AxA} signal was amplified using GFP-Booster Atto488 (Chromotek).

DAPI area as a measure of cell cycle position

To identify G2 cells in experiment presented in Figure 6 we synchronised cells in early S phase (by double Thymidine block), G2 phase (by double Thymidine block and 7h of release), late G2 (by an overnight treatment with RO3306 (Roche)) or left them asynchronous. Using these synchronized populations we established a cut-off for DAPI area size of G2 cells for each experiment. Following image acquisition, thresholding parameters selecting isolated DAPI areas were manually adjusted using ImageJ software. Subsequently, these parameters were propagated to all data sets, and an average DAPI area of each cell cycle stage was determined. Cells were identified as G2 if DAPI area was at least two standard deviations above the average DAPI area size of the S phase population. We confirmed that these values completely overlapped to the averages of DAPI area size coming from G2 synchronized populations (double thymidine released or RO3306 treated). All cells that had an equal or smaller DAPI area size from average values of S phase population were excluded from the analysis.

Supplemental References

Bailey, A.O., Panchenko, T., Sathyan, K.M., Petkowski, J.J., Pai, P.-J., Bai, D.L., Russell, D.H., Macara, I.G., Shabanowitz, J., Hunt, D.F., et al. (2013). Posttranslational modification of CENP-A influences the conformation of centromeric chromatin. Proc. Natl. Acad. Sci. *110*, 11827–11832.

Barnhart, M.C., Kuich, P.H.J.L., Stellfox, M.E., Ward, J.A., Bassett, E.A., Black, B.E., and Foltz, D.R. (2011). HJURP is a CENP-A chromatin assembly factor sufficient to form a functional de novo kinetochore. J. Cell Biol. *194*, 229–243.

Bodor, D.L., Rodríguez, M.G., Moreno, N., and Jansen, L.E.T. (2012). Analysis of Protein Turnover by Quantitative SNAP-Based Pulse-Chase Imaging. Curr. Protoc. Cell Biol. *Chapter 8*, Unit8.8.

Foltz, D.R., Jansen, L.E.T., Bailey, A.O., Yates, J.R., Bassett, E. a., Wood, S., Black, B.E., and Cleveland, D.W. (2009). Centromere-specific assembly of CENP-a nucleosomes is mediated by HJURP. Cell *137*, 472–484.

Khandelia, P., Yap, K., and Makeyev, E. V (2011). Streamlined platform for short hairpin RNA interference and transgenesis in cultured mammalian cells. Proc. Natl. Acad. Sci. U. S. A. *108*, 12799–12804.

Müller, S., Montes de Oca, R., Lacoste, N., Dingli, F., Loew, D., Almouzni, G., Montes de Oca, R., Lacoste, N., Dingli, F., Loew, D., et al. (2014). Phosphorylation and DNA Binding of HJURP Determine Its Centromeric Recruitment and Function in CenH3(CENP-A) Loading. Cell Rep. *8*, 190–203.

Rappsilber, J., Mann, M., and Ishihama, Y. (2007). Protocol for micro-purification, enrichment, pre-fractionation and storage of peptides for proteomics using StageTips. Nat. Protoc. *2*, 1896–1906.

Silva, M.C.C., Bodor, D.L., Stellfox, M.E., Martins, N.M.C., Hochegger, H., Foltz, D.R., and Jansen, L.E.T. (2012). Cdk Activity Couples Epigenetic Centromere Inheritance to Cell Cycle Progression. Dev. Cell *22*, 52–63.

Wang, L.-H., Li, D.-Q., Fu, Y., Wang, H.-P., Zhang, J.-F., Yuan, Z.-F., Sun, R.-X., Zeng, R., He, S.-M., and Gao, W. (2007). pFind 2.0: a software package for peptide and protein identification via tandem mass spectrometry. Rapid Commun. Mass Spectrom. *21*, 2985–2991.

Zasadzińska, E., Barnhart-Dailey, M.E.C., Kuich, P.H.J.L., and Foltz, D.R. (2013). Dimerization of the CENP-A assembly factor HJURP is required for centromeric nucleosome deposition. EMBO J. *32*, 2113–2124.